© 2021. Published by The Company of Biologists Ltd | Development (2021) 148, dev194969. doi:10.1242/dev.194969

RESEARCH ARTICLE

Ceramides mediate positional signals in *Arabidopsis thaliana* protoderm differentiation

Kenji Nagata[1], Toshiki Ishikawa[2], Maki Kawai-Yamada[2], Taku Takahashi[3] and Mitsutomo Abe[1,4,*]

ABSTRACT

The differentiation of distinct cell types in appropriate patterns is a fundamental process in the development of multicellular organisms. In *Arabidopsis thaliana*, protoderm/epidermis differentiates as a single cell layer at the outermost position. However, little is known about the molecular nature of the positional signals that achieve correct epidermal cell differentiation. Here, we propose that very-long-chain fatty acid-containing ceramides (VLCFA-Cers) mediate positional signals by stimulating the function of ARABIDOPSIS THALIANA MERISTEM LAYER1 (ATML1), a master regulator of protoderm/epidermis differentiation, during lateral root development. We show that VLCFA-Cers, which are synthesized predominantly in the outermost cells, bind to the lipid-binding domain of ATML1. Importantly, this cell type-specific protein-lipid association alters the activity of ATML1 protein and consequently restricts its expression to the protoderm/epidermis through a transcriptional feedback loop. Furthermore, establishment of a compartment, enriched with VLCFA-containing sphingolipids, at the outer lateral membrane facing the external environment may function as a determinant of protodermal cell fate. Taken together, our results indicate that VLCFA-Cers play a pivotal role in directing protoderm/epidermis differentiation by mediating positional signals to ATML1.

This article has an associated 'The people behind the papers' interview.

KEY WORDS: Epidermis, ATML1, VLCFA, Ceramide, Positional signal

INTRODUCTION

Sessile lifestyle imposes a bewildering array of biotic and abiotic stresses on vascular land plants. To defend against a hostile environment on land, plants have a specialized cell layer called the protoderm/epidermis at the interface between the plant body and the external environment. The protoderm/epidermis is a sheet-like tissue consisting of polarized protodermal/epidermal cells that synthesize and secrete surface lipids such as very-long-chain fatty acid (VLCFA) derivatives to form a protective hydrophobic layer known as the cuticle. The protodermal/epidermal cells adhere strongly to each other and protect the plant body from harmful invaders. Intact protodermal/epidermal cells are also crucial for shoot development. For example, loss of function of some *Arabidopsis* regulators involved in protodermal cell differentiation leads not only to a defective epidermis but also to a disorganized shoot apical meristem (SAM) structure (Abe et al., 2003; Johnson et al., 2005; Ogawa et al., 2015), indicating that intact protodermal cells communicate with inner cells to achieve the precise organization and function of the SAM.

Lateral root primordia (LRPs), which are post-embryonically generated from a subset of cells in the inner layer, develop the cuticularized outermost layer like other organs (Malamy and Benfey, 1997; Berhin et al., 2019; Torres-Martínez et al., 2019). *De novo* formation of the multi-layered structure of LRPs is carried out through tightly coordinated periclinal cell divisions. In the first periclinal cell division leading to Stage II LRPs, the plerome is laid down in the innermost layer, and in the second periclinal division to Stage III LRPs, the periblem is laid in the middle layer (Torres-Martínez et al., 2019). Subsequently, LRPs develop within this layered structure, and the outermost layer of Stage III LRPs eventually gives rise to the outermost layer of lateral roots (LRs), consisting of protodermal/epidermal cells and root cap cells. Thus, LRP development emerges as a good system with which to understand the molecular mechanism underlying the differentiation of protodermal/epidermal cells.

The protoderm/epidermis of aerial parts has previously been shown to be precisely marked by expression of *ARABIDOPSIS THALIANA MERISTEM LAYER1* (*ATML1*) and its closest paralog *PROTODERMAL FACTOR2* (*PDF2*), which encode HD-ZIP class IV transcription factors (TFs) (Lu et al., 1996; Sessions et al., 1999; Abe et al., 2003). ATML1 and PDF2 specifically bind to the L1 box, a well-conserved *cis*-regulatory element within the promoter region of shoot protoderm/epidermis-specific genes (Abe et al., 2001; 2003), and orchestrate a variety of protoderm/epidermis-specific events during shoot development. Thus, ATML1 and PDF2 act as master regulators of protodermal/epidermal cell differentiation in aerial parts (Abe et al., 2001, 2003; Ogawa et al., 2015), and dictate the location where the protodermal/epidermal identity manifests. Importantly, an L1 box is also found in the promoter of *ATML1* and *PDF2* (Abe et al., 2003). Consistent with this, the constitutive overexpression of ATML1 increases the transcript levels of endogenous *ATML1* and *PDF2* (Takada et al., 2013), and hypomorphic *atml1-1; pdf2-1* mutants show greatly decreased transcript levels of *ATML1* and *PDF2* relative to single mutants or wild-type plants (Ogawa et al., 2015). A transcriptional feedback loop therefore directs the transcription of *ATML1* and *PDF2*, although it remains puzzling how such autoregulation ultimately modulates the position-dependent expression of *ATML1* and *PDF2*.

Here, we report that *ATML1* and *PDF2* function redundantly as crucial regulators for protodermal cell differentiation during LRP development. Our data show that the outermost layer-specific activity of ATML1 is greatly influenced by VLCFAs, which have recently

[1]Department of Biological Sciences, Graduate School of Science, The University of Tokyo, 7-3-1, Hongo, Bunkyo-ku, Tokyo 113-0033, Japan. [2]Graduate School of Science and Engineering, Saitama University, 255 Shimo-Okubo, Saitama 338-8570, Japan. [3]Department of Biological Science, Graduate School of Natural Science and Technology, Okayama University, 3-1-1 Tsushimanaka, Okayama 700-8530, Japan. [4]Department of Life Sciences, Graduate School of Arts and Sciences, The University of Tokyo, 3-8-1, Komaba, Meguro-ku, Tokyo 153-8902, Japan.

*Author for correspondence (mabe@bio.c.u-tokyo.ac.jp)

M.A., 0000-0002-8423-1716

Handling Editor: Ykä Helariutta
Received 14 July 2020; Accepted 4 December 2020

Development (2021) 148, dev194969. doi:10.1242/dev.194969

been shown to be essential in various plant development processes (Bach et al., 2008; Markham et al., 2011; Trinh et al., 2019). Furthermore, we identify VLCFA-containing ceramides (VLCFA-Cers) as lipidic ligand candidates of ATML1 and demonstrate that VLCFA-Cers are essential components of the autoregulation loop controlled by ATML1 and PDF2. Based on our findings, we propose a novel molecular framework for the spatial control of protoderm/epidermis differentiation by a lipid-TF complex.

RESULTS

Novel function of *ATML1* and *PDF2* in LRP development

ATML1 and *PDF2* play crucial roles in embryonic and shoot development (Abe et al., 2003; Ogawa et al., 2015). However, whether *ATML1* and *PDF2* are also involved in root development has not been clarified. Thus, we first re-evaluated root phenotypes in the hypomorphic *atml1-1; pdf2-1* mutant.

In contrast to no apparent phenotype with the primary root including the radicles, the *atml1-1; pdf2-1* double mutant showed severe defects in LR formation (Fig. 1A; Fig. S1). Because no significant defects in the density of LRs and LRPs in 10-day-old *atml1-1; pdf2-1* seedlings were observed (Fig. S1), we next focused on LRP development. We determined the position of each LRP tip relative to the overlaying layers, which reflects the degree of progress of LRP development (Fig. 1B) (Malamy and Benfey, 1997; Casimiro et al., 2003), and evaluated the distribution of LRP tip locations in 10-day-old seedlings. The proportion of LRPs whose tips stayed at the pericycle layer was much higher in *atml1-1; pdf2-1* than in each single mutant and wild type (Fig. 1C). Because obvious phenotypes were not observed in LRP development of each single mutant (Fig. 1A,C; Fig. S1), we concluded that *ATML1* and *PDF2* play redundant and essential roles in the early stages of LRP development as well as shoot development.

To further understand the molecular function of these HD-ZIP class IV TFs in LRP development, we generated transgenic *Arabidopsis* plants, in the *atml1-3; pdf2-1* background, that expressed the *enhanced green fluorescent protein* (*EGFP*) fused to *ATML1* (*ATML1-EGFP*) under the control of native *ATML1* regulatory sequence (*gATML1-EGFP; atml1-3; pdf2-1*: Fig. S2) or the *PDF2-EGFP* under the control of native *PDF2* regulatory sequence (*gPDF2-EGFP; atml1-3; pdf2-1*: Fig. S2), and examined the expression pattern of *ATML1* and *PDF2* during LRP development. Whereas no EGFP fluorescence was detected in LRPs whose tips were positioned in the pericycle layer (Fig. 2A), ATML1-EGFP and PDF2-EGFP signals were detected in the nuclei of the outermost cells of LRPs whose tips were positioned in the endodermis layer (Fig. 2B). Subsequently, the fluorescence of ATML1-EGFP and PDF2-EGFP was observed in the outermost cells of LRPs and young LRs (Fig. 2C-E). According to the conventional model, when LRPs reach the endodermis layer (Stage III/Stage IV; Malamy and Benfey, 1997; Casimiro et al., 2003), the cell fate of the protoderm is determined (Torres-Martínez et al., 2019). Thus, the spatial and temporal expression patterns of ATML1-EGFP and PDF2-EGFP strongly suggest that these two TFs are appropriate markers for protodermal and root cap cell differentiation, and play a crucial role in initiating protoderm and root cap differentiation during LRP development.

Cell lineage- and cell position-dependent regulation

The above expression analysis revealed that *ATML1* and *PDF2* are expressed in the outermost cells during LRP development. However, our observations also showed that *ATML1* and *PDF2* are not expressed in the outermost cells after the first sloughing of root cap cells from LRs, even though these cells occupy the outermost cell position (Fig. 2F). This paradoxical observation led us to the idea that an outermost-cell position alone is not sufficient for the expression of *ATML1* and *PDF2*, and that their expression may also depend on cell lineage. Indeed, when we analyzed the expression of *ATML1* at other developmental stages and in other organs, stable *ATML1* expression was observed specifically in clonal outermost cells derived from the cells expressing *ATML1* at the one-cell embryonic stage (Takada and

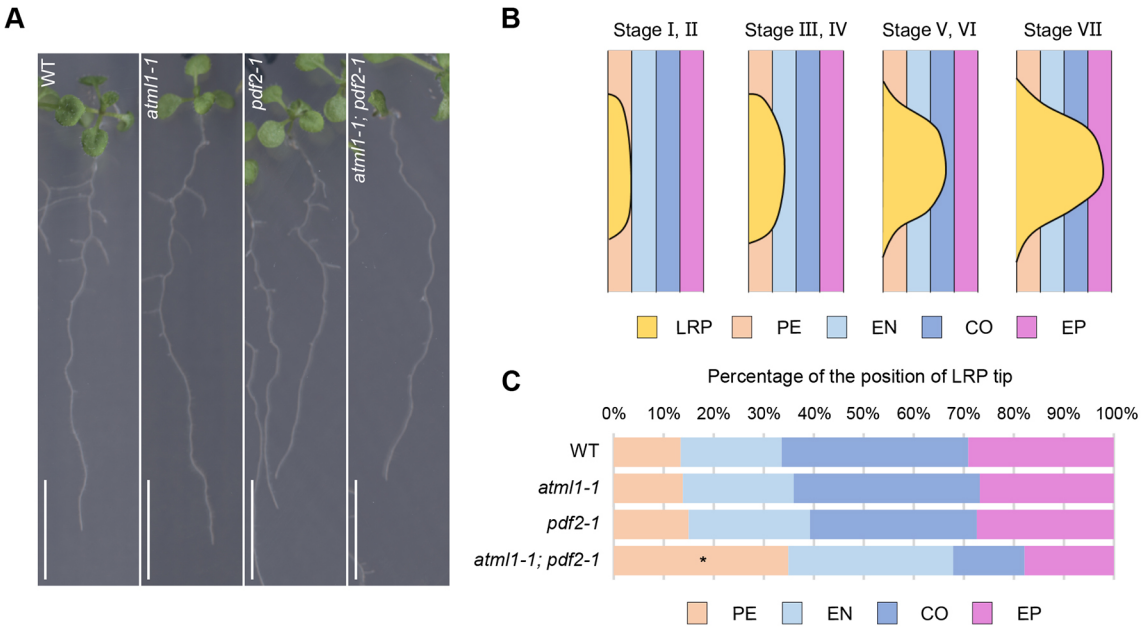

Fig. 1. *ATML1* and *PDF2* are redundantly involved in LRP development. (A) Seedlings of wild type (WT), *atml1-1*, *pdf2-1* and *atml1-1; pdf2-1* 10 days after germination. Scale bars: 1 cm. (B) Schematic representation of the LRP with the tip positioned in the PE, EN, CO and EP layers. The developmental stage of LRP corresponding to the position of the LRP tip is shown above (Casimiro et al., 2003). (C) Percentage of LRPs with tips positioned in the PE, EN, CO or EP layer in wild type, *atml1-1*, *pdf2-1* and *atml1-1; pdf2-1* (*P<0.05, Student's *t*-test, n=10). PE, pericycle; EN, endodermis; CO, cortex; EP, epidermis.

Development (2021) 148, dev194969. doi:10.1242/dev.194969

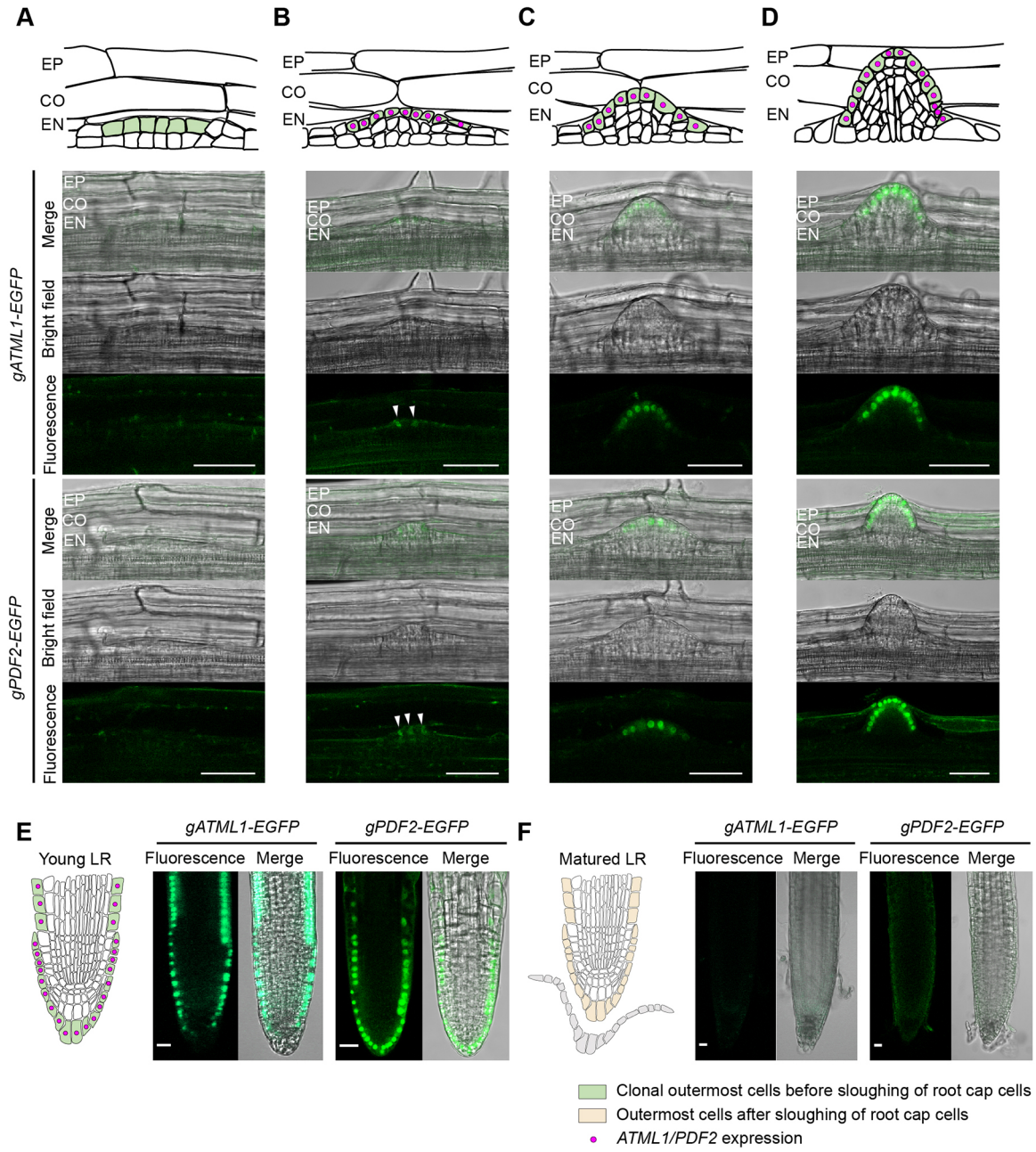

Fig. 2. Expression of *gATML1-EGFP* and *gPDF2-EGFP* during LRP development. (A-F) Fluorescence images of *gATML1-EGFP; atml1-3; pdf2-1* and *gPDF2-EGFP; atml1-3; pdf2-1* plants. (A) LRP with its tip positioned in the PE layer, (B) LRP with its tip positioned in the EN layer, (C) LRP with its tip positioned in the CO layer, (D) LRP with its tip positioned in the EP layer, (E) a young LR before sloughing of root cap cells and (F) a matured LR after sloughing of root cap cells. Representative drawings are shown above or next to the microscope images. White arrowheads in B indicate weak fluorescence signals in the outermost cell layer. Scale bars: 50 µm in A-D; 20 µm in E,F.

Jurgens, 2007), but was not detected in the outermost cells of the primary root after the loss of cell lineage (i.e. after sloughing of root cap cells from LRs) (Fig. S3).

In a lineage-based cell-fate decision mechanism, cell fate is restricted early in development and passed on to descendent cells (Scheres, 2001). Considering the autoregulation-dependent transcription of *ATML1* and *PDF2*, ATML1 and PDF2 proteins can be passed on via cell division as cell-fate determinants, conferring the cell-lineage dependence of their expression. In a position-dependent cell-fate decision mechanism, by contrast, cell fate can be flexibly changed according to cell position (Scheres, 2001). Because the epidermal differentiation of inner cells has been shown to be strictly inhibited even when these cells are descendants of the epidermal cell (Stewart and Dermen, 1975), it seems likely that an unidentified candidate signal may modulate the inheritance or function of ATML1 and PDF2 proteins according to cell position.

To test this assumption, we used a heat-inducible transient expression system, by the *HEAT SHOCK PROTEIN 18.2* (*HSP*) promoter (Takahashi et al., 1992), for the induction of *ATML1^{WT}-EGFP* and *NLS-mCherry* (*HSP::NLS-mCherry; HSP::ATML1^{WT}-EGFP*) in LR cells (Fig. 3A,B). Heat-pulse induction of the transcription of both *ATML1^{WT}-EGFP* and *NLS-mCherry* was confirmed by RT-PCR analysis (Fig. S4A). The ubiquitous expression of NLS-mCherry as a control indicated that transcription

Development (2021) 148, dev194969. doi:10.1242/dev.194969

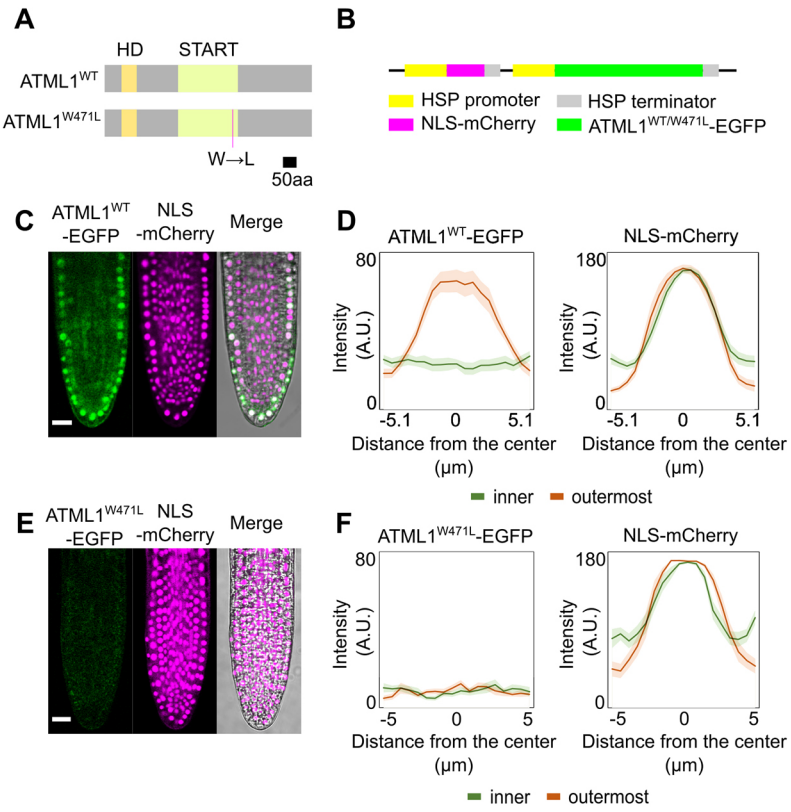

Fig. 3. ATML1 protein stability requires an outermost cell position, an outermost cell lineage and an intact lipid-binding START domain. (A) Representation of wild-type ATML1 (top) and ATML1^{W471L} (bottom) protein structure. HD, homeodomain; START, START domain. Magenta line indicates the mutation site. (B) Representation of the constructs used to visualize the post-translational behavior of NLS-mCherry, ATML1^{WT}-EGFP and ATML1^{W471L}-EGFP by a heat pulse-induced transient-overexpression system. (C,E) Fluorescence images of EGFP (left) and mCherry (middle), and merged fluorescence and bright-field image (right) in LRs before sloughing of root cap cells 2-3 h after heat-pulse treatment. (D,F) Plots of EGFP (left) and mCherry (right) intensity in inner cells and outermost cells (see also Fig. S5). *HSP::NLS-mCherry; HSP::ATML1^{WT}-EGFP* plants are shown in C,D; *HSP::NLS-mCherry; HSP::ATML1^{W471L}-EGFP* plants are shown in E,F. Data are mean±s.e.m. Scale bars: 20 µm in C,E.

from the *HSP* promoter and subsequent translation was successfully induced in all LR cells (Fig. 3C,D; Figs S4B and S5A,B). ATML1-EGFP was also induced in all cells of LR immediately after induction (Fig. S4B). However, in contrast to mCherry, EGFP fluorescence was detected specifically in the nuclei of the outermost cells 2-3 h after heat induction, but not in those of the inner cells (Fig. 3C,D; Fig. S5A,B). Moreover, ATML1^{WT}-EGFP fluorescence was not observed in the outermost cells of LR after the first sloughing of root cap cells from LR (Figs S5A,E and S6). These results indicate the existence of an unidentified candidate signal that relays the information of cell position and lineage, affects ATML1 function, and is therefore required to maintain *ATML1* expression.

Association between the lipid-binding domain and position-dependent stability of ATML1

HD-ZIP class IV family proteins, which are expressed predominantly in protodermal/epidermal cells, are characterized by a steroidogenic acute regulatory protein-related lipid-transfer (START) domain (Fig. 3A) (Ariel et al., 2007). Intriguingly, START domains from ATML1 and PDF2 have been shown to post-translationally stimulate TF activity via lipid-protein interactions in yeast (Schrick et al., 2014). To identify amino acids conserved among HD-ZIP class IV TFs, we compared the sequences of START domains of HD-ZIP class IV TFs with those of HD-ZIP class III TFs, which are also characterized by a START domain (Ariel et al., 2007), and identified several amino acids that are conserved only in HD-ZIP class IV TFs (Fig. S7A). In addition, to validate the importance of the identified amino acids in lipid binding, we compared the amino acid sequences of the START domains of ATML1 and PDF2 with the known ligand contact site of mammalian START domains (Fig. S7B) (Roderick et al., 2002; Schrick et al., 2014). Based on these sequence alignments, the W471 residue of ATML1 protein exhibits strong similarity with the ligand contact site of mammalian START domains (Fig. S7B). Thus, we focused on W471 as a putative lipid contact site in ATML1.

To examine the functional significance of the W471 residue in post-translational regulation of ATML1, we introduced a W471L point mutation into ATML1 based on a recent study (Schrick et al., 2014), and generated transgenic plants harboring the heat-inducible system of *ATML1^{W471L}-EGFP* and *NLS-mCherry* (*HSP::NLS-mCherry; HSP::ATML1^{W471L}-EGFP*) (Fig. 3A,B). In these plants, a single pulse of heat treatment induced the expression of ATML1^{W471L}-EGFP and NLS-mCherry in young LR immediately after heat-pulse treatment (Fig. S4C,D). In contrast to ATML1^{WT}-EGFP, transient induction of ATML1^{W471L}-EGFP in young LRs resulted in no fluorescence even in the outermost cells 2-3 h after heat induction (Fig. 3E,F; Fig. S5A,C). These observations indicate that W471 is crucial for the unidentified signal-mediated modulation of ATML1 protein in the outermost cells.

Involvement of VLCFA-Cers in the autoregulated maintenance of *ATML1* and *PDF2* expression

In order to screen for potential lipid species that interact with the ATML1 START domain as a component of the unidentified signaling pathway, we performed *in vitro* protein-lipid binding assays and found that the recombinant Glutathione S-transferase (GST) tagged START domain of ATML1 binds to VLCFA-Cers, ceramide-1-phosphates, phosphatidic acids, phosphatidylserines and several phosphatidylinositol phosphates (Fig. 4A; Fig. S8A,C). Interestingly, further evaluation of the effect of the W471L mutation revealed that the W471L mutation specifically attenuates the interaction between GST-START and VLCFA-Cers (Fig. 4A-C; Fig. S8A,B).

To determine whether the post-translational regulation of ATML1 is affected by VLCFA-Cers, we treated *HSP::NLS-mCherry; HSP::ATML1^{WT}-EGFP* seedlings with cafenstrole, an inhibitor of VLCFA

Development (2021) 148, dev194969. doi:10.1242/dev.194969

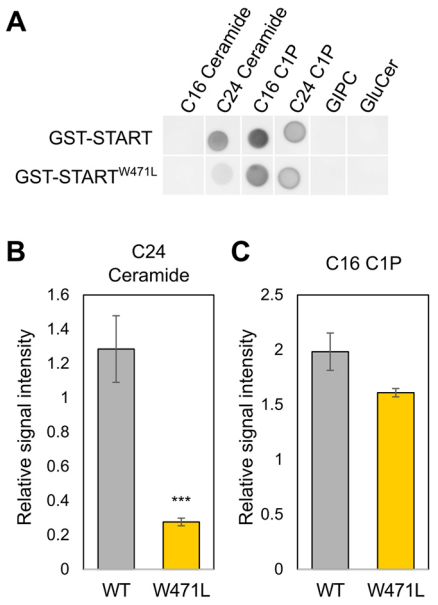

Fig. 4. VLCFA-Cers, the interaction of which with ATML1 is strongly disrupted by a W471L mutation, are strong candidate lipidic ligands of ATML1. (A) Interaction of the GST-tagged START domain of ATML1 (GST-START) and ATML1^{W471L} (GST-START^{W471L}) with various sphingolipids observed using a protein-lipid overlay (PLO) assay. C16 C1P, C16 ceramide-1-phosphate; C24 C1P, C24 ceramide-1-phosphate; GIPC, glycosyl inositol phosphoceramide; GluCer, glucosylceramide. (B,C) Relative signal intensity of protein-lipid interactions observed using the PLO assay (A). Signal intensity was measured using ImageJ software and compared with that of C24 C1P as a control. Data are mean±s.e.m (***P<0.01, Student's t-test; n=5 for PLO assay using GST-START; n=3 for PLO assay using GST-START^{W471L}).

biosynthesis (Nobusawa and Umeda, 2012). Consistently, 0.3 µM cafenstrole treatment strongly affected levels of VLCFA-containing sphingolipids, including ceramides (Fig. S9A-D). In *HSP::NLS-mCherry; HSP::ATML1^{WT}-EGFP* seedlings treated with 0.3 µM cafenstrole, the fluorescence of ATML1^{WT}-EGFP was significantly attenuated in the outermost cells of young LRs 2-3 h after heat induction (Fig. 5A,B; Fig. S5A,D), confirming that the stability of ATML1 protein is affected by VLCFA-Cers. Moreover, the same treatment strongly reduced both the fluorescence intensity of EGFP and the number of outermost cells expressing ATML1-EGFP in *gATML1-EGFP; atml1-3; pdf2-1* seedlings (Fig. S10).

To further examine whether the modulation of ATML1 stability by VLCFA-Cers is involved in the autoregulated transcription of *ATML1* and *PDF2*, we analyzed the link between sphingolipid metabolism and their mRNA levels. Consistent with the function of ATML1 and PDF2 as positive regulators of their own expression, cafenstrole treatment strongly reduced the amounts of *ATML1* and *PDF2* mRNAs (Fig. 5C). Fumonisin B1 (FB1), although it is known to induce programmed cell death, can inhibit the activity of ceramide synthases that preferentially use VLCFA as a substrate (Markham et al., 2011). Seedlings grown in the presence of FB1 at 0.5 µM, which is a moderate but effective concentration (Markham et al., 2011) (Fig. S9E-H), also greatly reduced the mRNA levels of both genes (Fig. S11).

Characterization of the VLCFA synthesis site

To strengthen the idea that VLCFA-Cers are essential components of the autoregulated pathway that controls protodermal/epidermal cell differentiation in cooperation with ATML1, we analyzed the expression pattern of PASTICCINO2 (PAS2), an essential enzyme for VLCFA biosynthesis (Bach et al., 2008). First, we confirmed that transgenic *Arabidopsis*, which express *PAS2-EGFP* under the control of native regulatory sequence of *PAS2* (*gPAS2-EGFP*), can rescue *pas2-3* from embryonic lethality (Fig. S2), indicating that PAS2-EGFP expression reflects the pattern of endogenous *PAS2* expression. The EGFP fluorescence was detected in the outermost cells of LRPs whose tips were positioned in the pericycle layer (Fig. 6A), suggesting that VLCFA production precedes the expression of *ATML1* and *PDF2*. However, the expression pattern of PAS2-EGFP was very similar to that of *ATML1* and *PDF2* in LRs and other tissues (Fig. 6B-E; Fig. S12), consistent with the presence of an L1-box sequence in the *PAS2* promoter (Nobusawa et al., 2013). In addition, a previous study has shown that gene silencing of *ATML1* and *PDF2* downregulates the mRNA levels of VLCFA

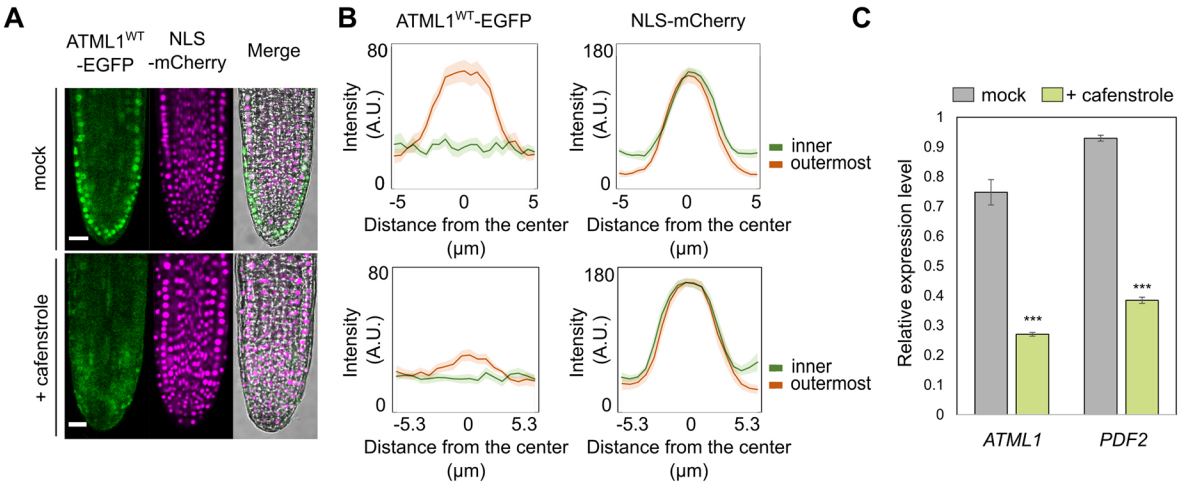

Fig. 5. VLCFA-Cers regulate ATML1 stability and are involved in the expression of *ATML1*/*PDF2* as lipidic ligands of ATML1. (A) Fluorescence images of EGFP (left) and mCherry (middle), and merged fluorescence and bright-field image (right) in LRs of *HSP::NLS-mCherry; HSP::ATML1^{WT}-EGFP* plants before sloughing of root cap cells 2-3 h after heat-pulse treatment. Seedlings were grown for 8 days on MS medium without (mock; top panels) or with (bottom panels) 0.3 µM cafenstrole. Scale bars: 20 µm. (B) Plots of EGFP (left) and mCherry (right) intensity in inner cells and outermost cells in A (see also Fig. S5). Mock treatment (top panels) and 0.3 µM cafenstrole treatment (bottom panels). Data are mean±s.e.m. (C) Relative expression levels of *ATML1* and *PDF2* in wild-type seedlings grown for 5 days on MS medium without (mock) or with 0.3 µM cafenstrole. Data are mean±s.e.m. (***P<0.01, Student's t-test, n=3).

Development (2021) 148, dev194969. doi:10.1242/dev.194969

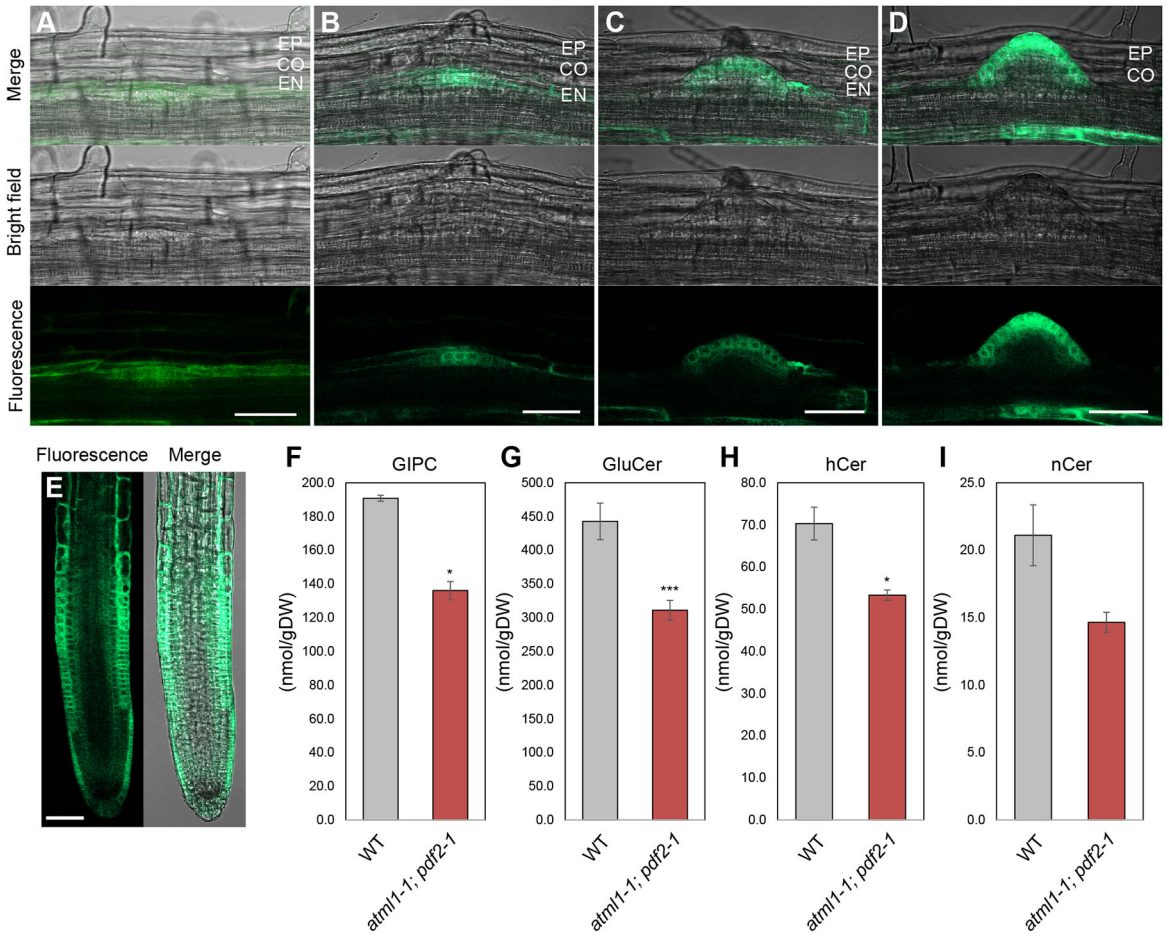

Fig. 6. Outermost cells are the primary site of VLCFA-Cer production. (A-E) Expression of *gPAS2-EGFP* during LRP development. (A) LRP with its tip positioned in the PE layer, (B) LRP with its tip positioned in the EN layer, (C) LRP with its tip positioned in the CO layer, (D) LRP with its tip positioned in the EP layer and (E) emerged LR. Scale bars: 50 µm in A-D; 20 µm in E. (F-I) Amount of VLCFA-containing sphingolipid in wild-type and *atml1-1; pdf2-1* seedlings grown for 10 days on MS medium. (F) VLCFA-containing GIPC, (G) VLCFA-containing GluCer, (H) hydroxy VLCFA-containing ceramide and (I) non-hydroxy VLCFA-containing ceramide. Data are mean±s.e.m. (***P<0.01, *P<0.05, Student's t-test, n=3).

biosynthesis-related genes, including *PAS2* (Rombolá-Caldentey et al., 2014). These results suggest that VLCFA-containing sphingolipid biosynthesis is initiated before the expression of *ATML1* and *PDF2*, but maintained in the outermost cells mainly via transcriptional activation of biosynthesis genes by a positive-feedback loop involving ATML1 and PDF2. Consistent with this, several sphingolipid pools in viable hypomorphic *atml1-1; pdf2-1* plants showed a significant decrease in VLCFAs (Fig. 6F-I).

VLCFA-containing sphingolipids mediate compartmentation of the outer lateral membrane

Sphingolipids are essential components of the cell membrane and are known to be embedded in lipid microdomains. Lipid microdomains play an important role in various cellular processes, including signal transduction and membrane trafficking (Simons and Ikonen, 1997; Simons and Toomre, 2000; Surma et al., 2012). In mammalian polarized epithelial cells, lipid microdomain-based apical sorting and trafficking results in sphingolipid-rich apical membrane compartmentation (Fig. 7A) (Simons and Ikonen, 1997; Simons and Toomre, 2000; Surma et al., 2012). Similarly, the plasma membrane of plant protodermal/epidermal cells in embryos, shoots and roots is also known to be highly polarized and compartmentalized (Fig. 7A-C) (Watanabe et al., 2004; Luo et al., 2007; Liao and Weijers, 2018; Nakamura and Grebe, 2018). Previous studies have demonstrated that some membrane proteins, such as the ATP-binding-cassette transporter WBC11, are located exclusively in the outer lateral membrane (Fig. 7B) (Luo et al., 2007), whereas we found that Remorin1.2 (REM1.2) (Jarsch et al., 2014) is localized to the inner lateral membrane of the LRP protodermal cells (Fig. 7C). To analyze the role of VLCFA-containing sphingolipids in the outer-inner polarity of plant LRP protodermal cells, we analyzed the localization of GFP-WBC11 and YFP-REM1.2 in LRP protodermal cells in presence of FB1. Surprisingly, the localization of GFP-WBC11 was affected in LRP protodermal cells of seedlings treated with FB1, but that of YFP-REM1.2 was not (Fig. 7B,C). Therefore, VLCFA-containing sphingolipids probably play a role in establishing the identity of protodermal/epidermal cells as integral constituents of the outer lateral membrane.

DISCUSSION

In *Arabidopsis*, the importance of cell position, rather than cell lineage, in determining cell fate is widely accepted (Stewart and Dermen, 1975; van den Berg et al., 1995; Scheres, 2001; Leyser and Day, 2009). In contrast, our analysis showed that both outermost cell lineage and outermost cell position contribute to *ATML1/PDF2*-mediated differentiation of protoderm/epidermis, and thus we propose that VLCFA-Cers are essential components of cell lineage- and position-dependent positional signaling.

Development (2021) 148, dev194969. doi:10.1242/dev.194969

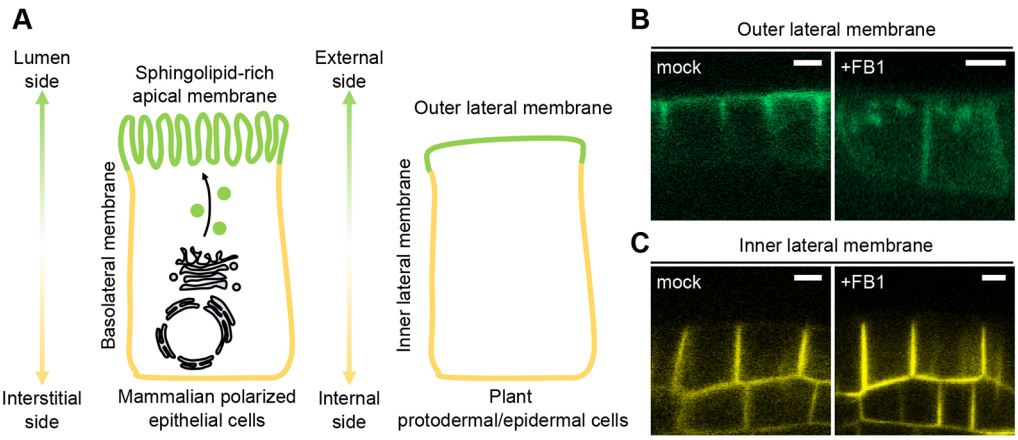

Fig. 7. VLCFA-containing sphingolipids are strongly associated with the outer lateral membrane of outermost cells. (A) Representation of the membrane compartmentation in mammalian epithelial cells (left) and plant protodermal/epidermal cells (right). (B) Fluorescence images of GFP in the protodermal cells of LRP of *proWBC11::GFP-WBC11* plants treated with mock (left) or 3 µM fumonisin B1 (FB1) (right) for 24 h. (C) Fluorescence images of YFP in the protodermal cells of LRP of *proREM1.2::YFP-REM1.2* plants treated with mock (left) or 3 µM FB1 (right) for 24 h. Scale bars: 5 µm.

Our analysis revealed that an unidentified candidate signal directs position-dependent post-translational regulation of ATML1 protein. It has been shown that plant subepidermal cells, which derive from asymmetric periclinal divisions of epidermal cells, develop according to their position rather than to their outermost cell lineage (Stewart and Dermen, 1975). Thus, even though the cells are directly derived from an outermost cell lineage, additional layers of regulation seem to prevent inheritance of the expression of *ATML1* and *PDF2* in an inner-cell position. Our assay in which ATML1 was induced by heat treatment revealed that ectopic ATML1 protein turns over more rapidly in inner cells than in outermost cells. This is consistent with our observations in 16-cell stage *gATML1-EGFP; atml1-3; pdf2-1* embryos, the inner cells of which are directly derived from outermost cells. In the majority of 16-cell-stage embryos, ATML1-EGFP fluorescence was limited to the outermost cells (Fig. S3E), although EGFP fluorescence was sometimes observed in the inner cells (Fig. S3D). Considering the tight repression of transcription from the *ATML1* promoter in the inner cells of 16-cell stage embryos (Takada and Jurgens, 2007), it seems that, even though ATML1-EGFP is passed on to inner cells, the protein disappears from these cells without activating the transcription of *ATML1-EGFP*. Taken together, we propose that the post-translational regulation of ATML1 protein observed in this study represents the position-based cell fate decision that prevents ectopic protoderm/epidermis differentiation in inner cells derived from outermost lineage cells.

Such inner cells derived from outermost lineage cells are generated through the asymmetric cell division (ACD) of outermost cells. ACD is a common mechanism for generating cell fate diversity. In *Arabidopsis*, BREAKING OF ASYMMETRY IN THE STOMATAL LINEAGE (BASL), which is embedded in the plasma membrane distal to the future division plane of a meristemoid mother cell, is a key regulator in the assignment of asymmetric cell fate via ACD in the stomatal cell lineage (Dong et al., 2009; Zhang et al., 2015, 2016). The polarized localization of BASL is stabilized by its phosphorylation, which is regulated by a mitogen-activated protein kinase (MAPK) signaling cascade, and, in turn, phosphorylated BASL recruits the MAPK signaling as a scaffold. Thus, the BASL-MAPK signaling feedback loop is reinforced in a polarized manner, and hence MAPK signaling asymmetrically phosphorylates SPEECHLESS, an essential TF for stomatal differentiation.

As mentioned above, we showed that the ATML1 protein itself is segregated to both the inner and outermost cells after the periclinal asymmetric division of outermost cells (Fig. S3C-E). Given that asymmetric cell fate assignment through ACD in the protodermal cell lineage is similar to that in the stomatal cell lineage, the unidentified candidate signaling component that controls post-translational regulation of ATML1 protein may be asymmetrically localized in the plasma membrane before ACD of eight-cell stage embryos. In our present work, VLCFA-Cers, which are lipidic ligand candidates of ATML1, emerge as the unidentified candidate signaling components that are asymmetrically localized in the plasma membrane, although this will remain speculative until the authentic lipid species that interact with the ATML1 protein *in vivo* are identified. Because of the highly redundant role of *ATML1* and *PDF2* in plant development and the high amino acid sequence similarity (>92%) between the START domains of ATML1 and PDF2, PDF2 is predicted to interact with the same ligand as ATML1. Loss of VLCFAs or VLCFA-containing sphingolipids results in embryonic lethality (Bach et al., 2008; Beaudoin et al., 2009; Markham et al., 2011) and severe defects in LRP development (Roudier et al., 2010; Markham et al., 2011), similar to *atml1; pdf2* double mutants. These findings further support a model in which VLCFA-Cer interacts with ATML1 and PDF2.

In protodermal/epidermal cells, a small proportion of ATML1 is present in the cytoplasm (Iida et al., 2019). Thus, an interaction between ATML1 and membrane lipids may occur in the cytoplasm. In mammalian cells, several ceramide species are generated as signaling molecules by hydrolysis of sphingomyelin in the outer leaflet, and they interact with cytoplasmic target molecules via trans-bilayer movement (Stancevic and Kolesnick, 2010). In addition, the activity of sphingomyelinase (SMase) is commonly exerted in microdomains and regulated by microdomain composition (Silva et al., 2009). Our present work shows that VLCFA-sphingolipids are involved in the outer-inner polarity of protodermal/epidermal cells, suggesting that VLCFA-sphingolipids are embedded predominantly in the outer lateral membrane of protodermal/epidermal cells as microdomains similar to mammalian polarized epithelial cells. Taken together, the generation of VLCFA-Cers by an equivalent of SMase may take place in the VLCFA-sphingolipid-rich microdomains in the outer lateral membrane. In plant cells, glycosyl inositol phosphoceramide (GIPC) in the outer leaflet is a major sphingolipid of plasma

Development (2021) 148, dev194969. doi:10.1242/dev.194969

membranes (Cacas et al., 2016), and complete loss of GIPC results in embryonic lethality (Tartaglio et al., 2017). Although not yet identified, a GIPC-specific phospholipase C that is predominantly located in the outer lateral membrane of the outermost cells may be a good candidate for an additional key regulator in generating a ligand for ATML1 in a position-dependent manner (Fig. S13).

Based on our finding of an outermost cell-specific protein-lipid association, we can propose a working model regarding the molecular determination of outermost and inner cells during the radial patterning process (Fig. 8). Outer lateral membrane components of the outermost cells are not passed on to either inner daughter cells through periclinal divisions or outermost cells derived from inner lineages. As a result, VLCFA-Cers generated in VLCFA-sphingolipid-rich microdomains in the outer lateral membrane by an equivalent of SMase might relay positional information along the radial axis in plants.

The START domain is also conserved in HD-ZIP class III proteins, which are key TFs in vascular development and leaf polarity, although their functional significance remains unknown (Ariel et al., 2007). Given that the association between the START domain and the homeodomain is confined to the plant kingdom (Schrick et al., 2004), such a plant-specific lipid-protein complex that mediates positional signals might represent an inevitable evolutionary strategy for sessile plants.

MATERIALS AND METHODS

Plant materials and growth conditions

Columbia (Col) was used as wild-type *Arabidopsis* (*Arabidopsis thaliana*) in this study. *atml1-1*, *atml1-3* and *pdf2-1* have been described previously (Abe et al., 2003; Ogawa et al., 2015). SALK_117051, obtained from the Salk Institute Genomic Analysis Laboratory T-DNA insertion lines (http://signal.salk.edu), was backcrossed with wild type twice and named *pas2-3*. Primer for genotyping information is listed in Table S1.

gATML1-EGFP; atml1-3; pdf2-1 (#4), *gPDF2-EGFP; atml1-3; pdf2-1* (#3), *gPAS2-EGFP; pas2-3* (#16), *HSP::NLS-mCherry; HSP::ATML1^{WT}-EGFP* (#4) and *HSP::NLS-mCherry; HSP::ATML1^{W471L}-EGFP* (#1) transgenic *Arabidopsis* were generated in this study. The *proREM1.2::YFP-REM1.2* transgenic plant has been described previously (Jarsch et al., 2014) and was obtained from T. Ott (University of Freiburg, Germany) and M. Nagano (Ritsumeikan University, Japan). The *proWBC11::GFP-WBC11* transgenic plant (Luo et al., 2007) was obtained from X-Y. Chen (Chinese Academy of Sciences, China) and H. Tanaka (Meiji University, Japan). Plants were grown on soil or Murashige and Skoog (MS) solid medium supplemented with 1% sucrose at 23°C under long-day conditions (16 h light/8 h dark).

Plasmid construction

Sequences of the primer used in this study are shown in Table S2. All of the PCRs were performed using PrimeSTAR Max DNA Polymerase (Takara). To generate the mutated ATML1 (ATML1^{W471}), two truncated coding sequences of ATML1 with W471L mutation (ATML1m1 and ATML1m2) were amplified by PCR. The ATML1m1 fragment was amplified using the primer sets ATML1m1-F and ATML1m1-R, and the ATML1m2 fragment was amplified using the primer sets ATML1m2-F and ATML1m2-R. For the pRI201AN_ATML1^{W471L}, the resulting PCR products were cloned together into NdeI/SalI-digested pRI201AN vector (TaKaRa) using the In-Fusion HD Cloning Kit (TaKaRa). pRI201AN_ATML1^{W471L} was used as the PCR template for plasmid constructions in this study.

To construct plasmids for heat-pulse induction assay, the promoter region of *HSP18.2* gene was amplified by PCR with primers HSPp-F and HSPp-R. The protein coding sequences of *NLS-mCherry* (Primers: NLS-mCherry-F and NLS-mCherry-R), *ATML1* (Primers: ATML1-F and ATML1-R), *ATML1^{W471L}* (Primers: ATML1-F and ATML1-R) and *EGFP* (Primers: EGFP-F and EGFP-R) were amplified using appropriate templates by PCR. Subsequently, the PCR-amplified *HSP* promoter and *NLS-mCherry* were cloned together into PstI/SalI-digested pRI201AN vector using In-Fusion HD Cloning Kit to generate pRI201AN_HSP::NLS-mCherry::HSP ter. The PCR-amplified *HSP* promoter, *ATML1* and *EGFP* fragments were cloned

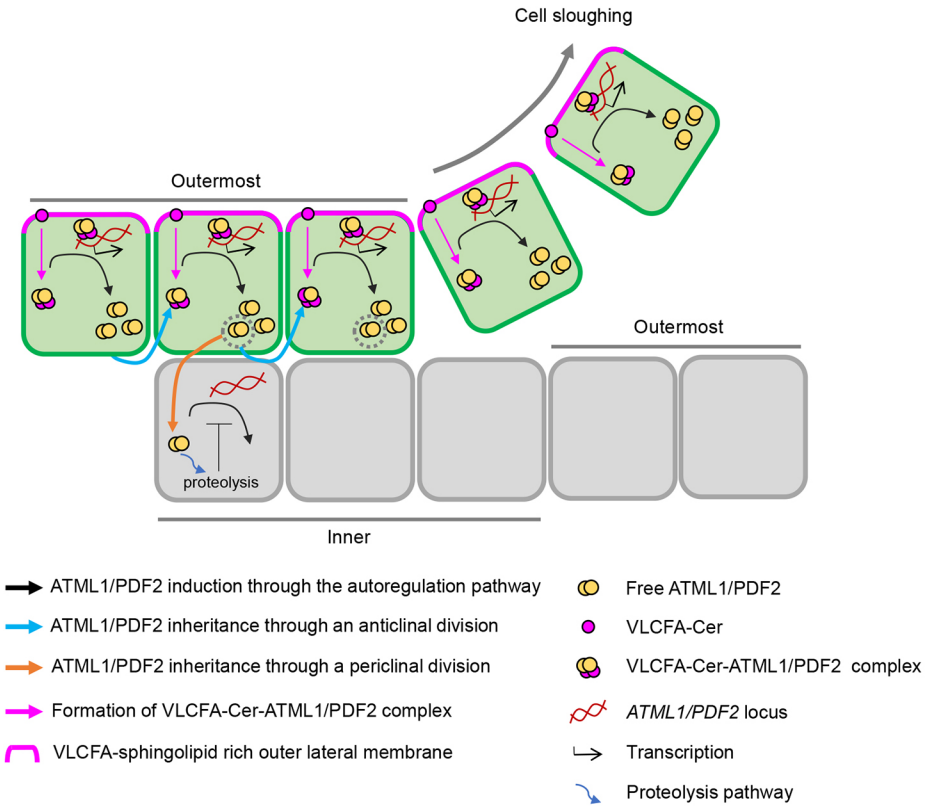

Fig. 8. Model of the molecular determination of outermost and inner cells. Model of the relationships between the position of the VLCFA-sphingolipid-rich outer lateral membrane, VLCFA-Cer-ATML1/PDF2 complex formation and the maintenance of *ATML1*/*PDF2* expression via autoregulation.

Development (2021) 148, dev194969. doi:10.1242/dev.194969

together into the PstI/SalI-digested pRI201AN vector to generate pRI201AN_HSP::ATML1-EGFP::HSP ter. The PCR-amplified *HSP* promoter, *ATML1*^{W471L}, and *EGFP* fragments were cloned together into PstI/SalI-digested pRI201AN vector to generate pRI201AN_HSP::ATML1^{W471L}-EGFP::HSP ter. Finally, the DNA fragments of HSP::ATML1-EGFP::HSP ter and HSP::ATML1^{W471L}-EGFP::HSP ter were amplified by PCR with primers HSP_ATML1_F and HSP_ATML1_R, and cloned into SmaI site of HSP::NLS-mCherry::HSP ter to generate *HSP::NLS-mCherry; HSP::ATML1*^{WT}*-EGFP* and *HSP::NLS-mCherry; HSP::ATML1*^{W471L}*-EGFP*, respectively.

To generate the *gATML1-EGFP* plasmid, the DNA fragment (5′-CACCAATAACTTCGTATAGCATACATTATACGAAGTTATGGATCCCGAATTCATAACTTCGTATAGCATACATTATACGAAGTTATT-3′) was inserted into pENTR/D-TOPO Vector (Thermo Fisher Scientific) according to the manufacturer's instructions (pENTR/D_loxP_BamHI-EcoRI_loxP). The sequences of *EGFP* (primers EGFP2-F and EGFP2-R) and the 3′ UTR sequence of *ATML1* (primers ATML1ter-F and ATML1ter-R) were then respectively amplified by PCR. The resulting PCR products were cloned together into EcoRI site of the pENTR/D_loxP_BamHI-EcoRI_loxP vector using the In-Fusion HD Cloning Kit to generate pENTR/D_loxP_BamHI-EcoRI-EGFP-ATML1 ter-loxP. Next, promoter and the protein-coding sequence of *ATML1* were amplified by PCR with primers gATML1-F and gATML1-R, and cloned into BamHI/EcoRI-digested pENTR/D_loxP_BamHI-EcoRI-EGFP-ATML1 ter-loxP (pENTR/D_loxP-gATML1-EGFP-loxP). Finally, for *gATML1-EGFP*, we recombined pENTR/D_loxP-gATML1-EGFP-loxP into the binary expression vector (pHGW.0) using Gateway LR Clonase II enzyme mix (Thermo Fisher Scientific).

To construct *gPDF2-EGFP*, we first respectively amplified the sequences of *EGFP* (primers EGFP3-F and EGFP3-R) and 3′ UTR sequence of *PDF2* (primers PDF2ter-F and PDF2ter-R) by PCR. The resulting PCR products were cloned together into BamHI/EcoRI-digested pENTR/D_loxP_BamHI-EcoRI_loxP vector using the In-Fusion HD Cloning Kit to generate pENTR/D_loxP_BamHI-EGFP-PDF2 ter-EcoRI-loxP. Next, promoter and the protein-coding sequence of *PDF2* were amplified by PCR with primers gPDF2-F and gPDF2-R, and cloned into the BamHI site of pENTR/D_loxP_BamHI-EGFP-PDF2 ter-EcoRI-loxP (pENTR/D_loxP-gPDF2-EGFP-loxP). Finally, for *gPDF2-EGFP*, we recombined pENTR/D_loxP-gPDF2-EGFP-loxP into a binary expression vector (pHGW.0) using the Gateway LR Clonase II enzyme mix.

To construct *gPAS2-EGFP*, we first amplified the sequence of *EGFP* by PCR (primers loxEGFP-F and loxEGFP-R) and cloned into the PstI/EcoRI-digested pRI201AN vector using the In-Fusion HD Cloning Kit (pRI201AN_loxP-EGFP-loxP). Next, the 3′ UTR sequence of *PAS2* was amplified by PCR with primers PAS2ter-F and PAS2ter-R, and cloned into the EcoRI site of pRI201AN_loxP-EGFP-loxP to generate pRI201AN_loxP-EGFP-PAS2 ter-loxP. Finally, for *gPAS2-EGFP*, the promoter and protein-coding sequence of *PAS2* were amplified by PCR (primers gPAS2-F and gPAS2-R), and cloned into the BamHI site of pRI201AN_loxP-EGFP-PAS2 ter-loxP.

To construct vectors for the protein expression, DNA fragments corresponding to the START domain of ATML1 and ATML1^{W471L} were amplified by PCR (primers START-F and START-R). The resulting PCR fragments were cloned into the NdeI/XbaI-digested pCold GST DNA (TaKaRa) to generate pCOLD_GST-START and pCOLD_GST-START^{W471L}, respectively.

Transformation of *Arabidopsis*

The constructs described above in binary vectors were introduced into *Agrobacterium tumefaciens* strain GV3101 and transformed into *Arabidopsis* plants by the floral-dip procedure (Clough and Bent, 1998).

Heat-pulse treatment and RT-PCR analysis

For induction of *HSP18.2* promoter activity, *Arabidopsis* seedlings were submerged into 1/2 MS liquid medium and incubated in a water bath for 3 h at 35°C. For RT-PCR analysis, total RNA was extracted using TRIzol reagent (Thermo Fisher Scientific) and was treated with RNase-free DNase (Thermo Fisher Scientific) according to the manufacturer's instructions. Total RNA (1 µg) was reverse transcribed with oligo dT primer according to the protocols of the Superscript II (Thermo Fisher Scientific). The primer sequence and PCR conditions are provided in Table S3.

Drug treatment

Both FB1 (Sigma-Aldrich) and cafenstrole (FUJIFILM Wako Pure Chemical Corporation) were dissolved in dimethyl sulfoxide (DMSO) and added to media so that the solvent concentration did not exceed 0.1% (v/v). For long-term treatment, seedlings were directly germinated on MS solid media supplemented with 0.5 µM FB1 or 0.3 µM cafenstrole. For FB1 short-term treatment, 7-day-old seedlings were transferred to 1/2 MS liquid media supplemented with 3 µM FB1 and incubated for 24 h. In each experiment, mock treatment [0.1% (v/v) DMSO treatment] was performed as a control experiment.

Microscopic analysis

Confocal microscopic analysis was performed using an LSM 510 Meta Confocal laser-scanning microscope (Carl Zeiss) or a C2 confocal Microscope (Nikon). All microscopic analyses were performed multiple times, and all repeats were successful.

Real-time RT-qPCR analysis

Total RNA was extracted from 5-day-old seedlings using TRIzol reagent and was treated with RNase-free DNase. Total RNA (1 µg) was reverse transcribed with oligo dT primer according to the protocols of the Superscript II.

RT-qPCR was performed with the Light Cycler 480 II (Roche) using Light Cycler 480 Probe Master (Roche). Three biological replicates were used for the quantification. The mean of housekeeping gene *PP2A* (AT1G13320) was used as an internal control to normalize the variability in expression levels. The primer sequence and probe list are provided in Table S4.

Lipid analysis and protein-lipid interaction analysis

Sphingolipid contents in lyophilized *Arabidopsis* tissues were determined using LC-MS/MS with a targeted monitoring method as described previously (Ishikawa et al., 2018). *Escherichia coli* Rosetta 2 strain (Novagen) expressing pCOLD_GST-START or pCOLD_GST-START^{W471L} constructs were grown in LB (Luria-Bertani) liquid medium till an OD600 of 0.4-0.6, and then transferred to an ice-cold water bath for 10 min. After 10 min incubation, cell cultures were incubated at 15°C for 30 min, and then the expression of GST tagged recombinant proteins was induced by 1 mM isopropyl-thiogalactoside (IPTG). After induction, cells were cultivated for 24 h at 15°C. Subsequently, the cells were harvested by centrifugation and the cell-pellet was resuspended in 10 ml of Bugbuster master mix and incubated at room temperature for 10 min. The cell suspension was centrifuged and the supernatant, which contains soluble GST-tagged recombinant proteins, was collected. GST-tagged recombinant proteins were purified using glutathione sepharose 4B (GE Healthcare) according to the manufacturer's instructions.

For the sphingolipids-protein interaction assay, sphingolipid-spotted membrane was originally prepared. C16 Ceramide (d18:1/16:0), C24 Ceramide (d18:1/24:0), C16 Ceramide-1-Phosphate (d18:1/16:0) and C24 Ceramide-1-Phosphate (d18:1/24:0) were purchased from Avanti Polar Lipids. Glucosylceramide from rice (Glucosylceramide mix) was purchased from Nagara Science. These lipids were dissolved in methanol/chloroform (1:1) to a concentration of 100 µM. GIPC fractions were prepared from *Arabidopsis* shoots by a method using isopropanol/hexane/water extraction, followed by fractionation with weakly anion exchange chromatography as described previously (Ishikawa et al., 2016). The purity of the GIPC fraction was determined by LC-MS/MS, in which no other sphingolipid classes were detected. The fraction was finally dissolved in 2-propanol/water/hexane (55:20:5) to a concentration of 100 µM. Aliquots of each lipid solution (2 µl) were directly spotted onto nitrocellulose membrane (Amersham Protran Supported 0.45 µm). For lipid-protein interaction assays other than those above, Sphingo Strips and PIP Strips were obtained from Echelon Biosciences. The lipid overlay assay was performed as described previously (Dowler et al., 2002). The membranes were blocked for 1 h at

room temperature in blocking buffer [2 mg/ml fatty-acid-free BSA, 150 mM NaCl, 50 mM Tris (pH 7.5), 0.1% (v/v) Tween 20]. The membranes were then incubated for 2 h at room temperature in the presence of 1 µg/ml purified GST tagged recombinant proteins. The membranes were probed with a polyclonal anti-GST antibody [MBL (PM013); 1:1000 in blocking buffer] for 1 h at room temperature. The secondary antibody, anti-rabbit IgG HRP-linked whole Ab donkey [GE Healthcare (NA934); 1:5000 in TBST], was incubated with the membrane for 1 h at room temperature. Bound antibody was visualized with the Ez West Lumi One (ATTO). The signals were collected using the Image Quant LAS 4000 mini (GE Healthcare). The mean of signal intensity was measured by using ImageJ software.

Acknowledgements
We thank A. Watanabe-Taneda and A. Imai for experimental assistance.

Competing interests
The authors declare no competing or financial interests.

Author contributions
Conceptualization: K.N., M.A.; Methodology: M.A.; Investigation: K.N., T.I., M.K.-Y., M.A.; Resources: K.N., M.A.; Writing - original draft: K.N., M.A.; Writing - review & editing: K.N., T.I., M.K.-Y., T.T., M.A.; Supervision: M.K.-Y., T.T., M.A.; Funding acquisition: K.N., M.A.

Funding
This work is supported by the Ministry of Education, Culture, Sports, Science and Technology (MEXT) [Grants-in-Aid for Scientific Research (C) 26440133 and 19K06703 to M.A.], by the NOVARTIS Foundation (Japan) for the Promotion of Science (37246 to M.A.) and by Japan Society for the Promotion of Science (19J12442 to K.N.).

Supplementary information
Supplementary information available online at
https://dev.biologists.org/lookup/doi/10.1242/dev.194969.supplemental

References
Abe, M., Takahashi, T. and Komeda, Y. (2001). Identification of a cis-regulatory element for L1 layer-specific gene expression, which is targeted by an L1-specific homeodomain protein. *Plant J.* **26**, 487-494. doi:10.1046/j.1365-313x.2001.01047.x

Abe, M., Katsumata, H., Komeda, Y. and Takahashi, T. (2003). Regulation of shoot epidermal cell differentiation by a pair of homeodomain proteins in *Arabidopsis*. *Development* **130**, 635-643. doi:10.1242/dev.00292

Ariel, F. D., Manavella, P. A., Dezar, C. A. and Chan, R. L. (2007). The true story of the HD-Zip family. *Trends Plant Sci.* **12**, 419-426. doi:10.1016/j.tplants.2007.08.003

Bach, L., Michaelson, L. V., Haslam, R., Bellec, Y., Gissot, L., Marion, J., Da Costa, M., Boutin, J.-P., Miquel, M., Tellier, F. et al. (2008). The very-long-chain hydroxy fatty acyl-CoA dehydratase PASTICCINO2 is essential and limiting for plant development. *Proc. Natl. Acad. Sci. USA* **105**, 14727-14731. doi:10.1073/pnas.0805089105

Beaudoin, F., Wu, X., Li, F., Haslam, R. P., Markham, J. E., Zheng, H., Napier, J. A. and Kunst, L. (2009). Functional characterization of the *Arabidopsis* β-ketoacyl-coenzyme a reductase candidates of the fatty acid elongase. *Plant Physiol.* **150**, 1174-1191. doi:10.1104/pp.109.137497

Berhin, A., de Bellis, D., Franke, R. B., Buono, R. A., Nowack, M. K. and Nawrath, C. (2019). The root cap cuticle: a cell wall structure for seedling establishment and lateral root formation. *Cell* **176**, 1367-1378.e8. doi:10.1016/j.cell.2019.01.005

Cacas, J.-L., Buré, C., Grosjean, K., Gerbeau-Pissot, P., Lherminier, J., Rombouts, Y., Maes, E., Bossard, C., Gronnier, J., Furt, F. et al. (2016). Revisiting plant plasma membrane lipids in tobacco: a focus on sphingolipids. *Plant Physiol.* **170**, 367-384. doi:10.1104/pp.15.00564

Casimiro, I., Beeckman, T., Graham, N., Bhalerao, R., Zhang, H., Casero, P., Sandberg, G. and Bennett, M. J. (2003). Dissecting *Arabidopsis* lateral root development. *Trends Plant Sci.* **8**, 165-171. doi:10.1016/S1360-1385(03)00051-7

Clough, S. J. and Bent, A. F. (1998). Floral dip: a simplified method for Agrobacterium-mediated transformation of *Arabidopsis thaliana*. *Plant J.* **16**, 735-743. doi:10.1046/j.1365-313x.1998.00343.x

Dong, J., MacAlister, C. A. and Bergmann, D. C. (2009). BASL controls asymmetric cell division in *Arabidopsis*. *Cell* **137**, 1320-1330. doi:10.1016/j.cell.2009.04.018

Dowler, S., Kular, G. and Alessi, D. R. (2002). Protein lipid overlay assay. *Sci. STKE* **2002**, pl6. doi:10.1126/stke.2002.129.pl6

Iida, H., Yoshida, A. and Takada, S. (2019). ATML1 activity is restricted to the outermost cells of the embryo through post-transcriptional repressions. *Development* **146**, dev169300. doi:10.1242/dev.169300

Ishikawa, T., Ito, Y. and Kawai-Yamada, M. (2016). Molecular characterization and targeted quantitative profiling of the sphingolipidome in *Rice*. *Plant J.* **88**, 681-693. doi:10.1111/tpj.13281

Ishikawa, T., Fang, L., Rennie, E. A., Sechet, J., Yan, J., Jing, B., Moore, W., Cahoon, E. B., Scheller, H. V. and Kawai-Yamada, M. (2018). GLUCOSAMINE INOSITOLPHOSPHORYLCERAMIDE TRANSFERASE1 (GINT1) is a GlcNAc-containing glycosylinositol phosphorylceramide glycosyltransferase. *Plant Physiol.* **177**, 938-952. doi:10.1104/pp.18.00396

Jarsch, I. K., Konrad, S. S. A., Stratil, T. F., Urbanus, S. L., Szymanski, W., Braun, P., Braun, K.-H. and Ott, T. (2014). Plasma membranes are subcompartmentalized into a plethora of coexisting and diverse microdomains in *Arabidopsis* and *Nicotiana benthamiana*. *Plant Cell* **26**, 1698-1711. doi:10.1105/tpc.114.124446

Johnson, K. L., Degnan, K. A., Ross Walker, J. and Ingram, G. C. (2005). AtDEK1 is essential for specification of embryonic epidermal cell fate. *Plant J.* **44**, 114-127. doi:10.1111/j.1365-313X.2005.02514.x

Leyser, O. and Day, S. (2009). *Mechanisms in Plant Development*: John Wiley & Sons.

Liao, C. Y. and Weijers, D. (2018). A toolkit for studying cellular reorganization during early embryogenesis in *Arabidopsis thaliana*. *Plant J.* **93**, 963-976. doi:10.1111/tpj.13841

Lu, P., Porat, R., Nadeau, J. A. and O'Neill, S. D. (1996). Identification of a meristem L1 layer-specific gene in *Arabidopsis* that is expressed during embryonic pattern formation and defines a new class of homeobox genes. *Plant Cell* **8**, 2155-2168. doi:10.1105/tpc.8.12.2155

Luo, B., Xue, X.-Y., Hu, W.-L., Wang, L.-J. and Chen, X.-Y. (2007). An ABC transporter gene of *Arabidopsis thaliana*, AtWBC11, is involved in cuticle development and prevention of organ fusion. *Plant Cell Physiol.* **48**, 1790-1802. doi:10.1093/pcp/pcm152

Malamy, J. E. and Benfey, P. N. (1997). Organization and cell differentiation in lateral roots of *Arabidopsis thaliana*. *Development* **124**, 33-44.

Markham, J. E., Molino, D., Gissot, L., Bellec, Y., Hématy, K., Marion, J., Belcram, K., Palauqui, J.-C., Satiat-Jeunemaître, B. and Faure, J.-D. (2011). Sphingolipids containing very-long-chain fatty acids define a secretory pathway for specific polar plasma membrane protein targeting in *Arabidopsis*. *Plant Cell* **23**, 2362-2378. doi:10.1105/tpc.110.080473

Nakamura, M. and Grebe, M. (2018). Outer, inner and planar polarity in the *Arabidopsis* root. *Curr. Opin. Plant Biol.* **41**, 46-53. doi:10.1016/j.pbi.2017.08.002

Nobusawa, T. and Umeda, M. (2012). Very-long-chain fatty acids have an essential role in plastid division by controlling z-ring formation in *Arabidopsis thaliana*. *Genes Cells* **17**, 709-719. doi:10.1111/j.1365-2443.2012.01619.x

Nobusawa, T., Okushima, Y., Nagata, N., Kojima, M., Sakakibara, H. and Umeda, M. (2013). Synthesis of very-long-chain fatty acids in the epidermis controls plant organ growth by restricting cell proliferation. *PLoS Biol.* **11**, e1001531. doi:10.1371/journal.pbio.1001531

Ogawa, E., Yamada, Y., Sezaki, N., Kosaka, S., Kondo, H., Kamata, N., Abe, M., Komeda, Y. and Takahashi, T. (2015). ATML1 and PDF2 play a redundant and essential role in *Arabidopsis* embryo development. *Plant Cell Physiol.* **56**, 1183-1192. doi:10.1093/pcp/pcv045

Roderick, S. L., Chan, W. W., Agate, D. S., Olsen, L. R., Vetting, M. W., Rajashankar, K. R. and Cohen, D. E. (2002). Structure of human phosphatidylcholine transfer protein in complex with its ligand. *Nat. Struct. Biol.* **9**, 507-511. doi:10.1038/nsb812

Rombolá-Caldentey, B., Rueda-Romero, P., Iglesias-Fernández, R., Carbonero, P. and Oñate-Sánchez, L. (2014). *Arabidopsis* DELLA and two HD-ZIP transcription factors regulate GA signaling in the epidermis through the L1 box cis-element. *Plant Cell* **26**, 2905-2919. doi:10.1105/tpc.114.127647

Roudier, F., Gissot, L., Beaudoin, F., Haslam, R., Michaelson, L., Marion, J., Molino, D., Lima, A., Bach, L., Morin, H. et al. (2010). Very-long-chain fatty acids are involved in polar auxin transport and developmental patterning in *Arabidopsis*. *Plant Cell* **22**, 364-375. doi:10.1105/tpc.109.071209

Scheres, B. (2001). Plant cell identity. The role of position and lineage. *Plant Physiol.* **125**, 112-114. doi:10.1104/pp.125.1.112

Schrick, K., Nguyen, D., Karlowski, W. M. and Mayer, K. F. X. (2004). START lipid/sterol-binding domains are amplified in plants and are predominantly associated with homeodomain transcription factors. *Genome Biol.* **5**, R41. doi:10.1186/gb-2004-5-6-r41

Schrick, K., Bruno, M., Khosla, A., Cox, P. N., Marlatt, S. A., Roque, R. A., Nguyen, H. C., He, C., Snyder, M. P., Singh, D. et al. (2014). Shared functions of plant and mammalian StAR-related lipid transfer (START) domains in modulating transcription factor activity. *BMC Biol.* **12**, 70-78. doi:10.1186/s12915-014-0070-8

Sessions, A., Weigel, D. and Yanofsky, M. F. (1999). The *Arabidopsis thaliana* MERISTEM LAYER 1 promoter specifies epidermal expression in meristems and young primordia. *Plant J.* **20**, 259-263. doi:10.1046/j.1365-313x.1999.00594.x

Silva, L. C., Futerman, A. H. and Prieto, M. (2009). Lipid raft composition modulates sphingomyelinase activity and ceramide-induced membrane physical alterations. *Biophys. J.* **96**, 3210-3222. doi:10.1016/j.bpj.2008.12.3923

Simons, K. and Ikonen, E. (1997). Functional rafts in cell membranes. *Nature* **387**, 569. doi:10.1038/42408

Simons, K. and Toomre, D. (2000). Lipid rafts and signal transduction. *Nat. Rev. Mol. Cell Biol.* **1**, 31-39. doi:10.1038/35036052

Stancevic, B. and Kolesnick, R. (2010). Ceramide-rich platforms in transmembrane signaling. *FEBS Lett.* **584**, 1728-1740. doi:10.1016/j.febslet.2010.02.026

Stewart, R. N. and Dermen, H. (1975). Flexibility in ontogeny as shown by the contribution of the shoot apical layers to leaves of periclinal chimeras. *Am. J. Bot.* **62**, 935-947. doi:10.1002/j.1537-2197.1975.tb14134.x

Surma, M. A., Klose, C. and Simons, K. (2012). Lipid-dependent protein sorting at the trans-Golgi network. *Biochim. Biophys. Acta* **1821**, 1059-1067. doi:10.1016/j.bbalip.2011.12.008

Takada, S. and Jurgens, G. (2007). Transcriptional regulation of epidermal cell fate in the *Arabidopsis* embryo. *Development* **134**, 1141-1150. doi:10.1242/dev.02803

Takada, S., Takada, N. and Yoshida, A. (2013). Induction of epidermal cell fate in *Arabidopsis* shoots. *Plant. Signal. Behav.* **8**, e26236. doi:10.4161/psb.26236

Takahashi, T., Naito, S. and Komeda, Y. (1992). The *Arabidopsis* HSP18.2 promoter/GUS gene fusion in transgenic *Arabidopsis* plants: a powerful tool for the isolation of regulatory mutants of the heat-shock response. *Plant J.* **2**, 751-761. doi:10.1111/j.1365-313X.1992.tb00144.x

Tartaglio, V., Rennie, E. A., Cahoon, R., Wang, G., Baidoo, E., Mortimer, J. C., Cahoon, E. B. and Scheller, H. V. (2017). Glycosylation of inositol phosphorylceramide sphingolipids is required for normal growth and reproduction in *Arabidopsis*. *Plant J.* **89**, 278-290. doi:10.1111/tpj.13382

Torres-Martínez, H. H., Rodríguez-Alonso, G., Shishkova, S. and Dubrovsky, J. G. (2019). Lateral root primordium morphogenesis in angiosperms. *Front. Plant. Sci.* **10**, 206. doi:10.3389/fpls.2019.00206

Trinh, D.-C., Lavenus, J., Goh, T., Boutté, Y., Drogue, Q., Vaissayre, V., Tellier, F., Lucas, M., Voß, U., Gantet, P. et al. (2019). PUCHI regulates very long chain fatty acid biosynthesis during lateral root and callus formation. *Proc. Natl. Acad. Sci. USA* **116**, 14325-14330. doi:10.1073/pnas.1906300116

van den Berg, C., Willemsen, V., Hage, W., Weisbeek, P. and Scheres, B. (1995). Cell fate in the *Arabidopsis* root meristem determined by directional signalling. *Nature* **378**, 62. doi:10.1038/378062a0

Watanabe, M., Tanaka, H., Watanabe, D., Machida, C. and Machida, Y. (2004). The ACR4 receptor-like kinase is required for surface formation of epidermis-related tissues in *Arabidopsis thaliana*. *Plant J.* **39**, 298-308. doi:10.1111/j.1365-313X.2004.02132.x

Zhang, Y., Wang, P., Shao, W., Zhu, J.-K. and Dong, J. (2015). The BASL polarity protein controls a MAPK signaling feedback loop in asymmetric cell division. *Dev. Cell* **33**, 136-149. doi:10.1016/j.devcel.2015.02.022

Zhang, Y., Guo, X. and Dong, J. (2016). Phosphorylation of the polarity protein BASL differentiates asymmetric cell fate through MAPKs and SPCH. *Curr. Biol.* **26**, 2957-2965. doi:10.1016/j.cub.2016.08.066

Table S1. List of primers used for genotyping assay.

Primer name	Forward primer (5' to 3')	Reverse primer (5' to 3')	Target sequence
P1 and P2	TCCAAAAATTGATAGGCATC	ATAAAGAAAAAAGCTTACCCG	*ATML1*
P3 and P4	GATCAGTGCCTTGAAGGAAA	CTGTTGTCGACATTGTTGTC	*PDF2*
P5 and P6	TGGGATATACAGGCAGAAGA	GTTTTGGAGCTACAGGGATCCAGA	*ATML1*
P7 and P8	GATCAGTGCCTTGAAGGAAA	ATCTTAGTTGTGGAATCATAC	*PDF2*
P9 and P10	ACATTCTCCTCCCATGGAAAC	TAGTACATGAACGAACAAGAC	*PAS2*
P11 and P12	AGGCGAGTGGTTCTTTGTTTT	TCACTCAACAACATCGAGCAC	*FLC*

Table S2. List of primers used for plasmid construction.

Name	Sequence (5' to 3')
ATML1m1-F	CACTGTTGATACATATGTATCATCCAAACATGTTC
ATML1m1-R	AGCCACCAAACGTTTTGCACCGAAAGCTAA
ATML1m2-F	AAACGTTTGGTGGCTACACTTGACCGCCAA
ATML1m2-R	ATTCAGAATTGTCGAGGCTCCGTCGCAGGCCAGAGC
HSPp-F	CCAAGCTTGCATGCCAAGCTTTTCTCTTCATTTCTC
HSPp-R	TGTTCGTTGCTTTTCGGGAGA
NLS-mCherry-F	GAAAAGCAACGAACACATATGCGACCCCCAAAGAAGAAG
NLS-mCherry-R	ATTCAGAATTGTCGATTACTTGTACAGCTCGTCCAT
ATML1-F	GAAAAGCAACGAACACATATGTATCATCCAAACATGTT
ATML1-R	ACTAGTGGCTCCGTCGCAGGCCAGAGC
EGFP-F	GACGGAGCCACTAGTATGGTGAGCAAGGGCGAGGAG
EGFP-R	ATTCAGAATTGTCGATTACTTGTACAGCTCGTCCAT
HSP_ATML1_F	CGGCCGCTGGATCCCAAGCTTTTCTCTTCATTTCTC
HSP_ATML1_R	TGATTACGAATTCCCCTTATCTTTAATCATATTCCA
EGFP2-F	TTATGGATCCCGAATTCGTGAGCAAGGGCGAGGAGCTGTT
EGFP2-R	AAACATCGATTACTTGTACAGCTCGTCCAT
ATML1ter-F	CAAGTAATCGATGTTTTCGGGTAAGCTTTTTT
ATML1ter-R	TACGAAGTTATGAATTTGATGACTTGGTCTCCATAATTTC
gATML1-F	ACGAAGTTATGGATCCAAGCTTAGTTTCTTATTTGACATA
gATML1-R	CCTTGCTCACGAATTCGGCTCCGTCGCAGGCCAGAGC
EGFP3-F	ACGAAGTTATGGATCCGTGAGCAAGGGCGAGGAGCTGTTC
EGFP3-R	TGAAAAAAAACTATTACTTGTACAGCTCGTCCATG
PDF2ter-F	GTAATAGTTTTTTTTCAGGTATGATTCC
PDF2ter-R	ACGAAGTTATGAATTCTTTACCTTTCTATGTTAGGCTGTTA
gPDF2-F	TACGAAGTTATGGATCCCATATAGTCCAACTTTGCAAGACAT
gPDF2-R	CCCTTGCTCACGGATCCCGCTCCTCCTCCAACATCACAAGAA
loxEGFP-F	CCAAGCTTGCATGCCATAACTTCGTATAGCATACATTATACGAAGTTATGGATCCGGTGGTGGTGGTGGTGTCGAC
loxEGFP-R	CCATGATTACGAATTATAACTTCGTATAATGTATGCTATACGAAGTTATGAATTCTTACTTGTACAGCTCGTCCAT
PAS2ter-F	GTACAAGTAAGAATTAAGAAAAGATTTAGAAAGAGACGAA
PAS2ter-R	ACGAAGTTATGAATTCAATTTCATAAATATTATTAAGAATCC
gPAS2-F	ACGAAGTTATGGATCCGGAATATCCACTGTTAGCTT
gPAS2-R	CACCACCACCGGATCCTTCCCTCTTGGATTTGGAGAG
START-F	AGGGCCCGGGACATATGATACCTTCTGAGGCTGATAAG
START-R	AGATTACCTATCTAGAACAAGCCGGAATGTTGCTGGC

Table S3. List of primers and PCR conditions used for RT-PCR analysis.

Gene	Forward primer (5' to 3')	Reverse primer (5' to 3')	annealing temp.	cycles
ATML1$^{WT/W471L}$*-EGFP*	TGGATGATCCGGGAAGACCT	CTCGCCCTTGCTCACCATAC	50	30
NLS-mCherry	GACCCCCAAAGAAGAAGCGTA	CTGCTTGATCTCGCCCTTCA	50	30
TUB2	CTCAAGAGGTTCTCAGCAGTA	TCACCTTCTTCATCCGCAGTT	50	30

Table S4. List of primers and probes used for RT-qPCR analysis.

Gene	Forward primer (5' to 3')	Reverse primer (5' to 3')	Probe
ATML1	GGAATAGTGTCTCCTTGCTTCG	TGATGCGTCCGTACAACTTT	122
PDF2	TCTCCTTGCTCCGAGTCAATA	TGCATCTGTACAGCTCTCTTGTAGA	106
PP2A	ATTCCGATAGTCGACCAAGC	AACATCAACATCTGGGTCTTCA	22

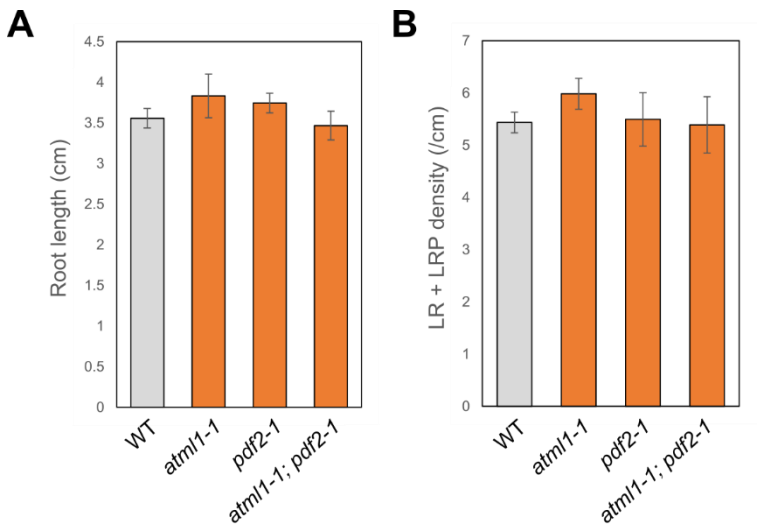

Fig. S1. Root phenotypes in the *atml1-1; pdf2-1* mutant.

(A) Primary root length of 10-day-old wild-type, *atml1-1*, *pdf2-1* and *atml1-1; pdf2-1* seedlings grown on MS medium. Data are mean ± SE values (n = 10). **(B)** Number of LRs and LRPs per root length in 10-day-old wild-type, *atml1-1*, *pdf2-1* and *atml1-1; pdf2-1* seedlings grown on MS medium. Data are mean ± SE values (n = 10).

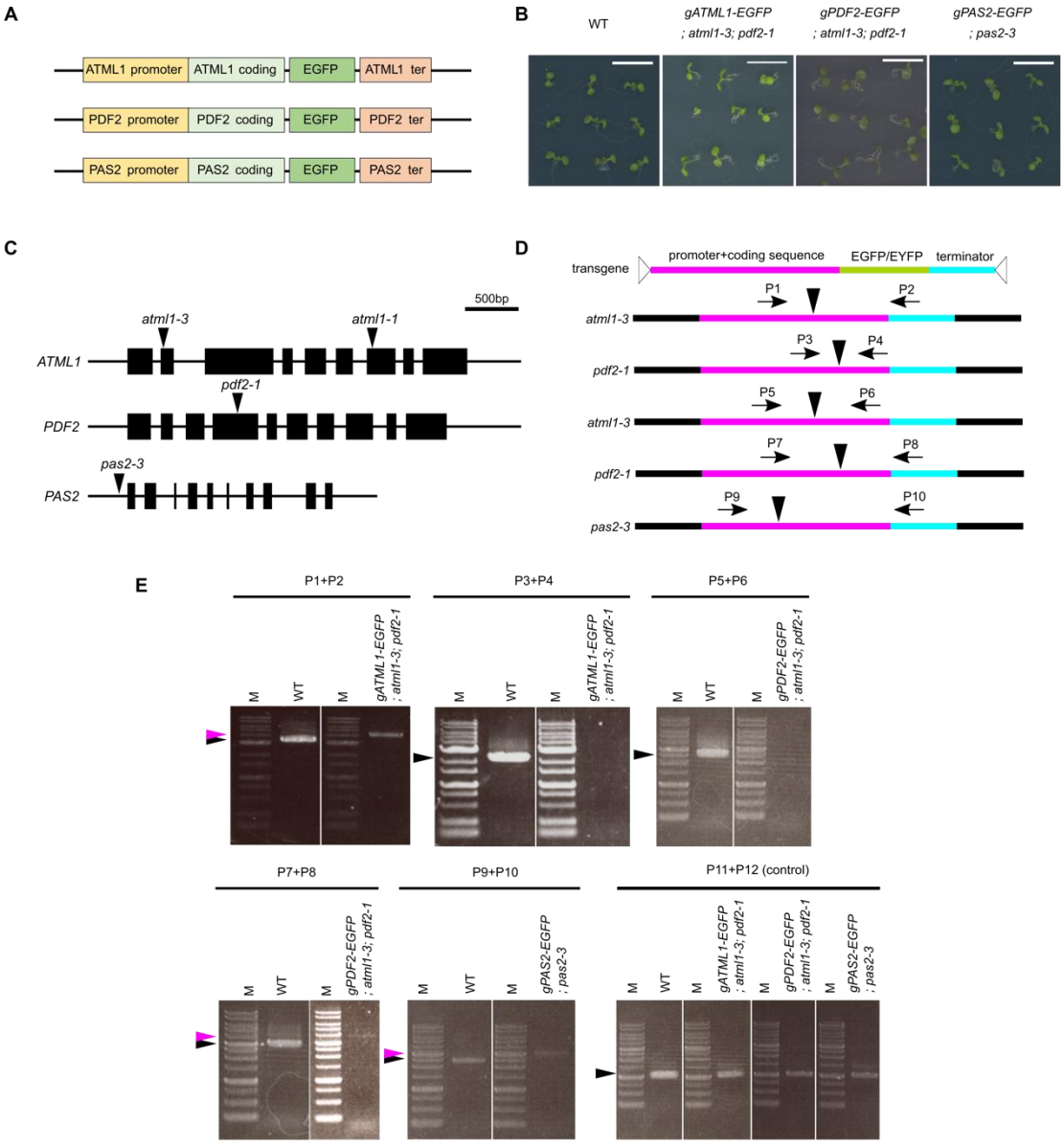

Fig. S2. Genetic complementation with reporter genes.

(A) Representation of plasmid constructions. **(B)** Phenotypes of 5-day-old seedlings. Wild type, *gATML1-EGFP; atml1-3; pdf2-1*, *gPDF2-EGFP; atml1-3; pdf2-1* and *gPAS2-EGFP; pas2-3* are shown (left to right). Scale bars: 1 cm. **(C)** Representation of T-DNA insertion sites in the mutants. **(D)** Primer design for confirmation of transgenes

in mutant background (primer information (P1-P10) are shown in Table S1). Arrows indicate primer locations and arrowheads indicate T-DNA insertion sites. **(E)** Genotyping assay. Black arrows indicate the expected amplicon size of the WT gene. As a control, *FLC* (AT5G10140) was amplified using primer set of P11 and P12 (Table S1). Magenta arrows indicate the expected amplicon size of the transgene. M: 1-kbp DNA ladder.

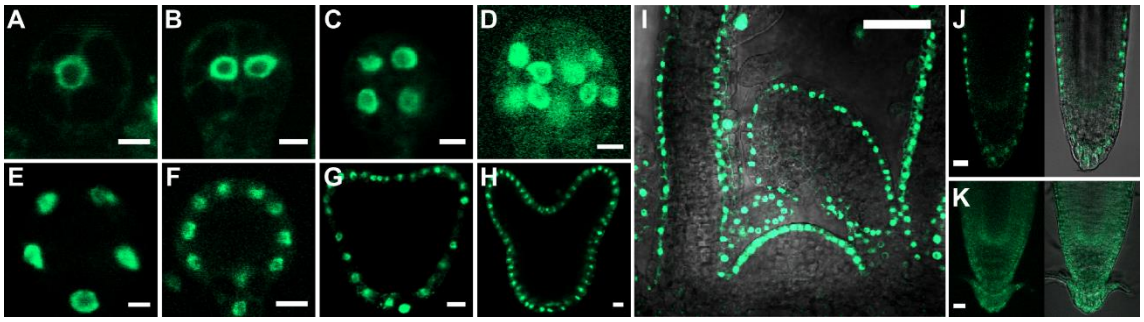

Fig. S3. Expression of *gATML1-EGFP* during embryogenesis.

(A) 1-cell stage embryo, **(B)** 2-cell stage embryo, **(C)** Octant (8-cell) stage embryo, **(D and E)** Two dermatogen (16-cell) stage embryos showing different fluorescence patterns, **(F)** Globular stage embryo, **(G)** Triangular stage embryo, **(H)** Heart stage embryo, **(I)** Shoot apical meristem and leaf primordia, **(J)** Radicle (Primary root before sloughing of the root cap cells) and **(K)** Primary root after sloughing of root cap cells. Scale bars: 5 µm in (A-E); 10 µm in (F-H); 20µm in (J, K); 50 µm in (I).

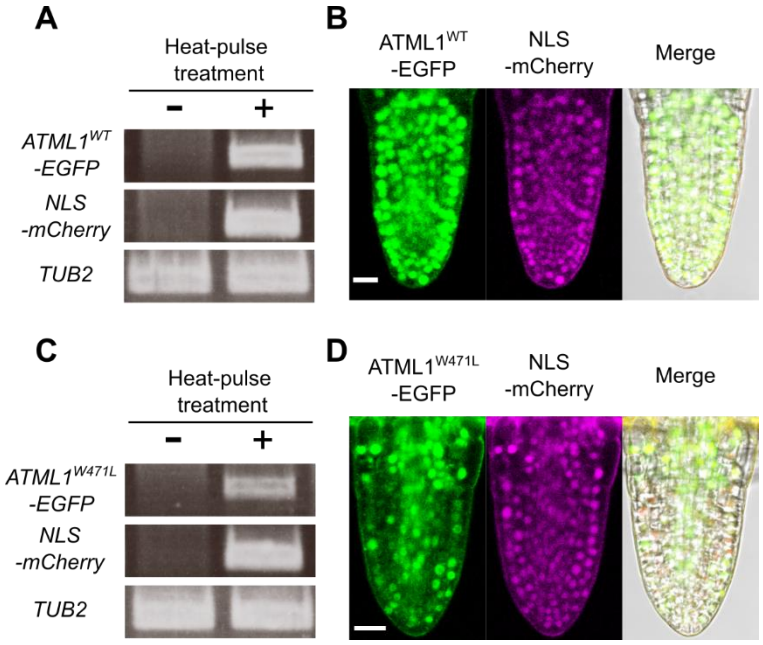

Fig. S4. Heat-pulse-dependent induction of transgene.

(A) *ATML1^{WT}-EGFP* and *NLS-mCherry* mRNA in *HSP::NLS-mCherry; HSP::ATML1^{WT}-EGFP* seedlings. **(B)** Fluorescence images of EGFP (left) and mCherry (middle), and merged fluorescence and bright field image (right) in LRs of *HSP::NLS-mCherry; HSP::ATML1^{WT}-EGFP* plants before sloughing of root cap cells immediately after heat-pulse treatment (0-30 min). **(C)** *ATML1^{W471L}-EGFP* and *NLS-mCherry* mRNA in *HSP::NLS-mCherry; HSP::ATML1^{W471L}-EGFP* seedlings. **(D)** Fluorescence images of EGFP (left) and mCherry (middle), and merged fluorescence and bright field image (right) in LRs of *HSP::NLS-mCherry; HSP::ATML1^{W471L}-EGFP* plants before sloughing of root cap cells immediately after heat-pulse treatment (0-30 min). For RT-PCR analysis,

whole seedlings were harvested for RNA extraction before (–) and after (+) heat-pulse treatment. *TUB2* (AT5G62690) was amplified as a control.

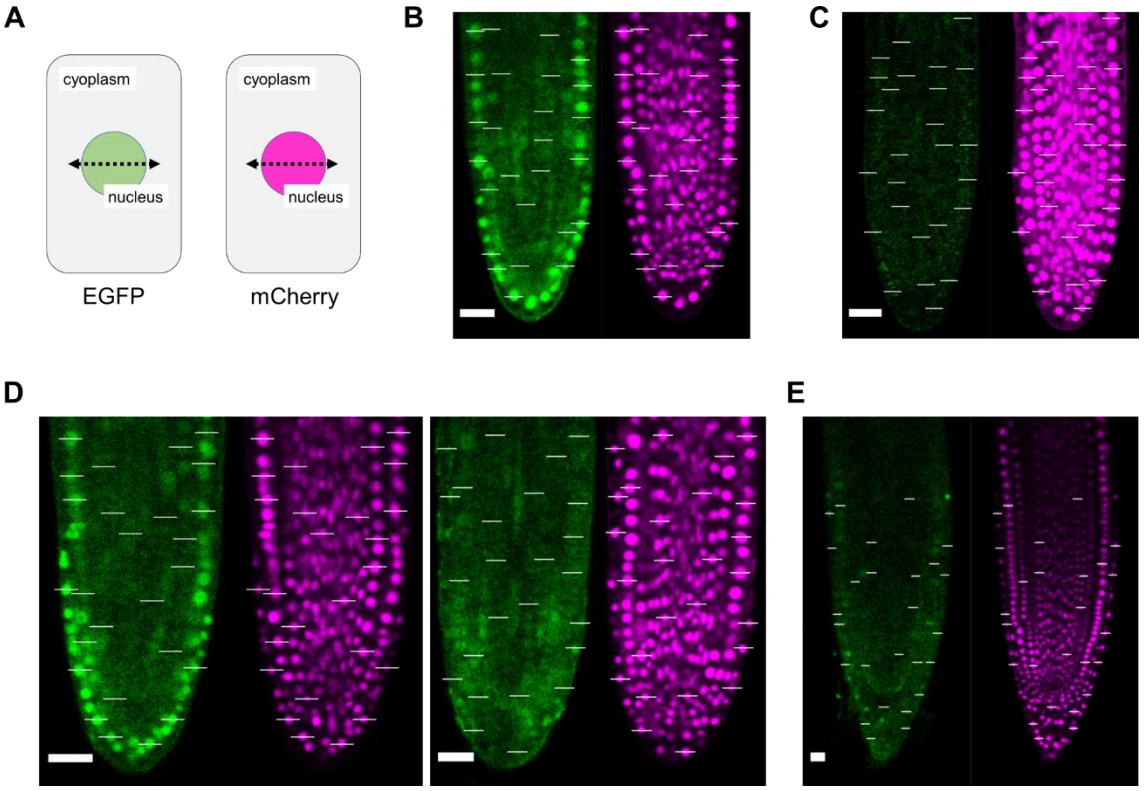

Fig. S5. Measuring the EGFP and mCherry intensity.

(A) Fluorescence intensities of EGFP and mCherry were measured by using the [Plot Profile] tools of ImageJ software. Intensity values of EGFP and mCherry were measured on the line crossing the nucleus of a single cell. **(B-E)** A series of intensity values was acquired from 13 inner cells and 13 outermost cells by using the fluorescence images in Fig. 3C, Fig. 3E, Fig 5A and Fig. S6A, corresponding to Fig. S5B, C, D and E, respectively. The lengths of the lines crossing the nucleus are the same in each pair of panels.

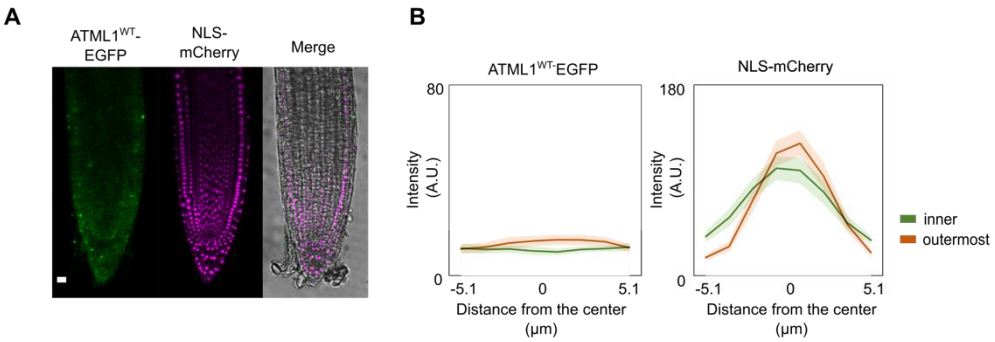

Fig. S6. Posttranslational regulation of ATML1 in LRs after sloughing of root cap cells.

(A) Fluorescence images of EGFP (left) and mCherry (middle), and merged fluorescence and bright field image (right) in LRs of *HSP::NLS-mCherry; HSP::ATML1^{WT}-EGFP* plants after sloughing of root cap cells 2–3 hours after heat-pulse treatment. Scale bars: 20 μm. **(B)** Plot of EGFP (left) and mCherry (right) intensity in inner cells and outermost cells in (A) (see Fig. S5).

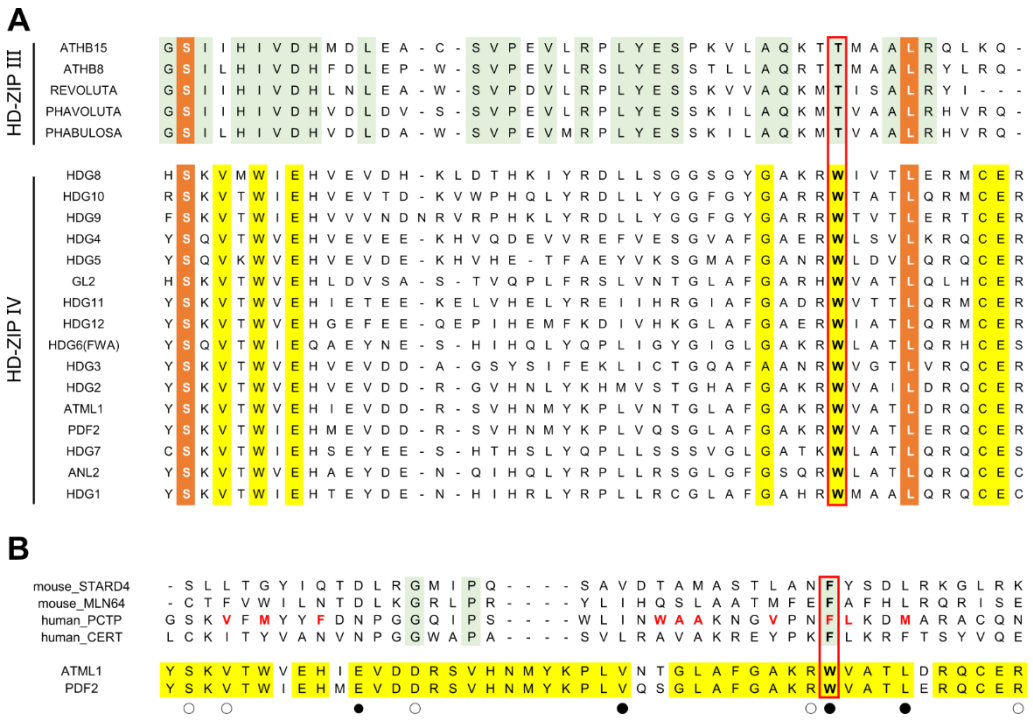

Fig. S7. Amino acid sequences of the START domain.

(A) Alignment of amino acid sequence of the C-terminal region of the START domain.

(B) Alignment of amino acid sequence of the C-terminal region of the START domain from ATML1, PDF2, STARD4, MLN64, PCTP, and CERT. Red font indicates ligand contact points, as derived from the PCTP-PtCho co-crystal. Red box indicates the amino acid targeted for site-directed mutagenesis of ATML1. Yellow background indicates amino acids conserved in HD-ZIP class IV proteins but not in HD-ZIP class III proteins (A), or conserved in ATML1 and PDF2, but not in mammalian proteins (B). Green background color indicates amino acids conserved in HD-ZIP class III proteins, but not in HD-ZIP class IV proteins (A), or in mammalian proteins but not in ATML1 or PDF2 (B). Orange background color indicates amino acids conserved among HD-ZIP class III

proteins and HD-ZIP class IV proteins. Open circles indicate a site where the amino acids exhibit weak similarity. Closed circles indicate a site where the amino acids exhibit strong similarity.

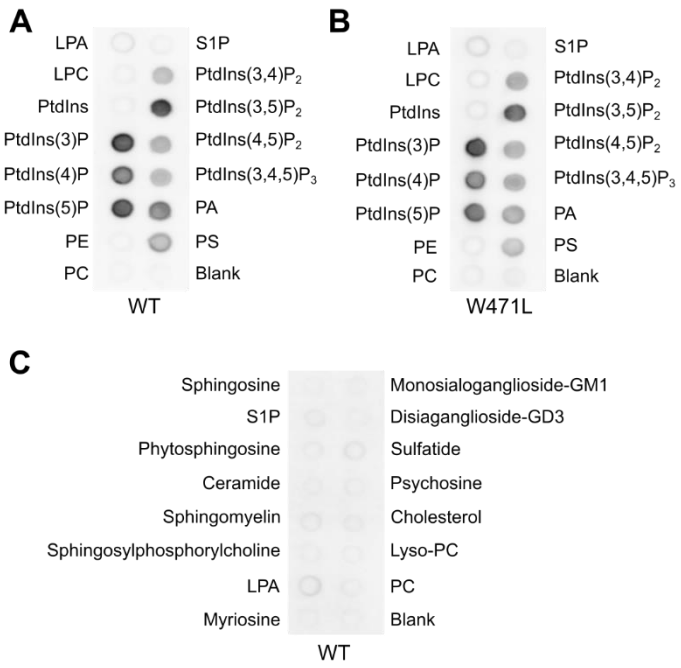

Fig. S8. Interaction of the GST tagged START domain of ATML1 (GST-START) and ATML1^{W471L} (GST-START^{W471L}) with various lipids.

(A and B) Interaction of GST-START (A) or GST-START^{W471L} (B) with all phosphoinositides and other biological important lipids. **(C)** Interaction of GST-START with various sphingolipids and other lipids. S1P, sphingosine 1-phosphate; LPA, lysophosphatidic acid; Lyso-PC, lysophosphatidylcholine; PC, phosphatidylcholine; LPA, lysophosphatidic acid; LPC, lysophosphocholine; PtdIns, phosphatidylinositol; PtdIns(3)P, phosphatidylinositol (3)-phosphate; PtdIns(4)P, phosphatidylinositol (4)-phosphate; PtdIns(5)P, phosphatidylinositol (5)-phosphate; PE, phosphatidylethanolamine; PtdIns(3,4)P2, phosphatidylinositol (3,4)-bisphosphate; PtdIns(3,5)P2, phosphatidylinositol (3,5)-bisphosphate; PtdIns(4,5)P2,

phosphatidylinositol (4,5)-bisphosphate; PtdIns(3,4,5)P3, phosphatidylinositol (3,4,5)-trisphosphate; PA, phosphatidic acid; PS, phosphatidylserine.

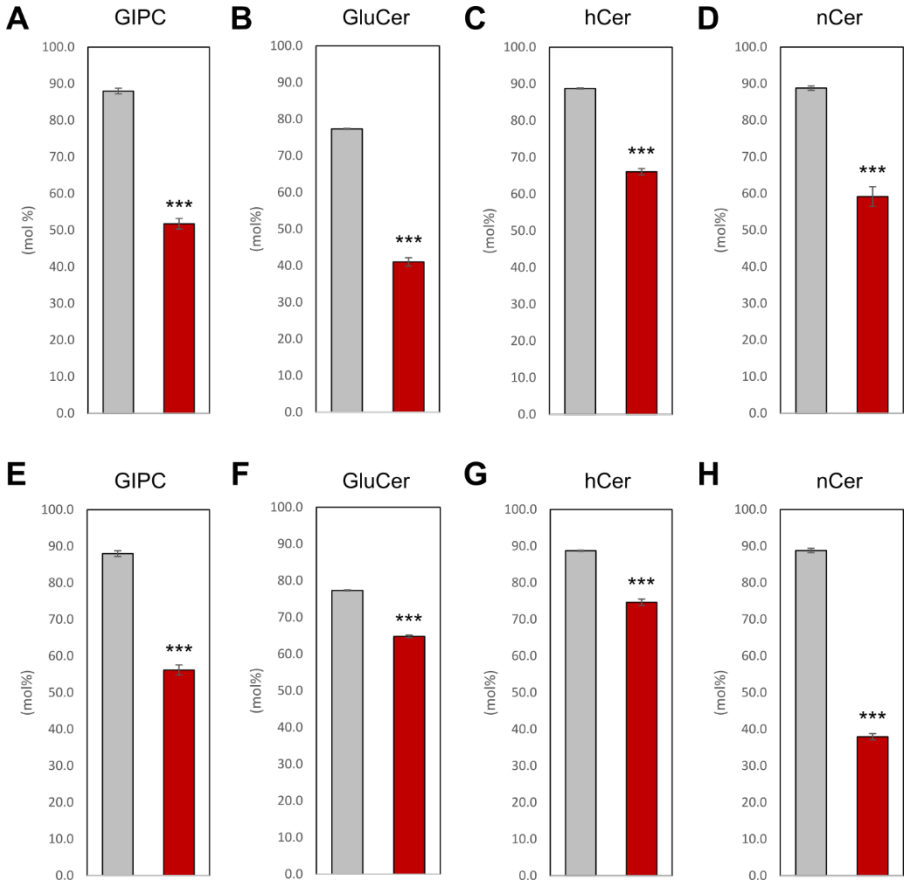

Fig. S9. Effect of cafenstrole and FB1 treatment on the sphingolipid metabolism.

The molar fraction of VLCFA-containing species in each sphingolipid class was measured in wild-type seedlings grown for 5 days in the presence of 0.3 µM cafenstrole **(A-D)** or 0.5 µM FB1 **(E-H).** (A, E), VLCFA-containing GIPC. (B, F), VLCFA-containing GluCer. (C, G) Hydroxy VLCFA containing ceramide. (D, H) Non-hydroxy VLCFA containing ceramide. Data are mean ± SE values (***$P < 0.01$, Student's *t* test, n = 3).

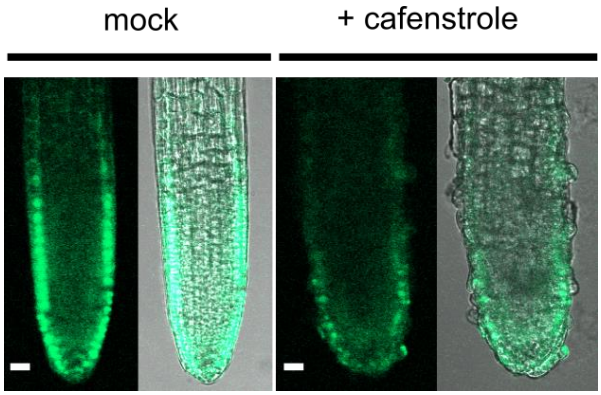

Fig. S10. Effect of cafenstrole treatment on the expression of *gATML1-EGFP*.

Shown are LRs before sloughing of root cap cells of *gATML1-EGFP; atml1-3; pdf2-1* plants grown for 8 days on MS medium without (mock) or with 0.3 µM cafenstrole. Scale bars: 20 µm.

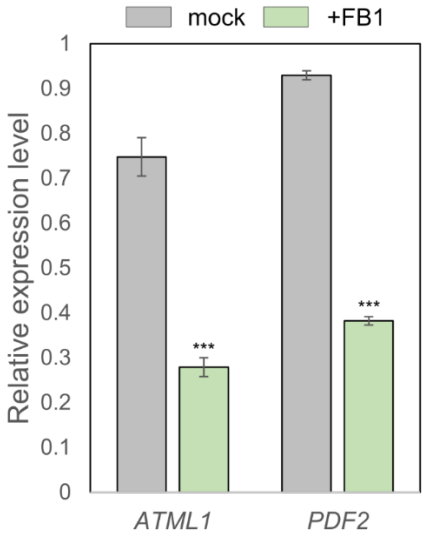

Fig. S11. Effect of the inhibition of ceramide synthase activity on the expression of *ATML1* and *PDF2*.

Relative expression levels of *ATML1* and *PDF2* in 5-day-old wild-type seedlings grown on MS medium without (mock) or with 0.5 µM FB1. Data are mean ± SE values (***$P < 0.01$, Student's *t* test, n = 3).

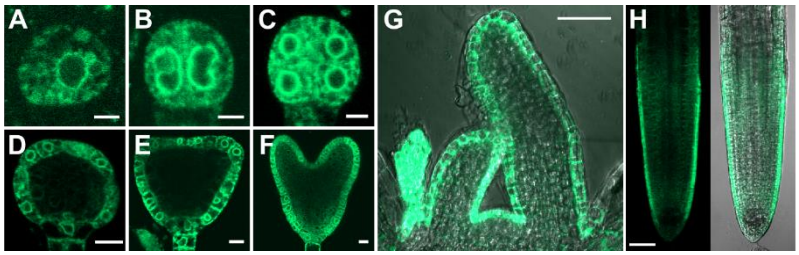

Fig. S12. Expression of *gPAS2-EGFP* during embryogenesis.

(A) 1-cell stage embryo, **(B)** 2-cell stage embryo, **(C)** Octant (8-cell) stage embryo, (**D)** Globular stage embryo, **(E)** Triangular stage embryo **(F)** Heart stage embryo, **(G)** Shoot apical meristem and leaf primordia and **(H)** Primary root. Scale bars: 5 µm in (A-C); 10 µm in (D-F); 20 µm in (H); 50 µm in (G).

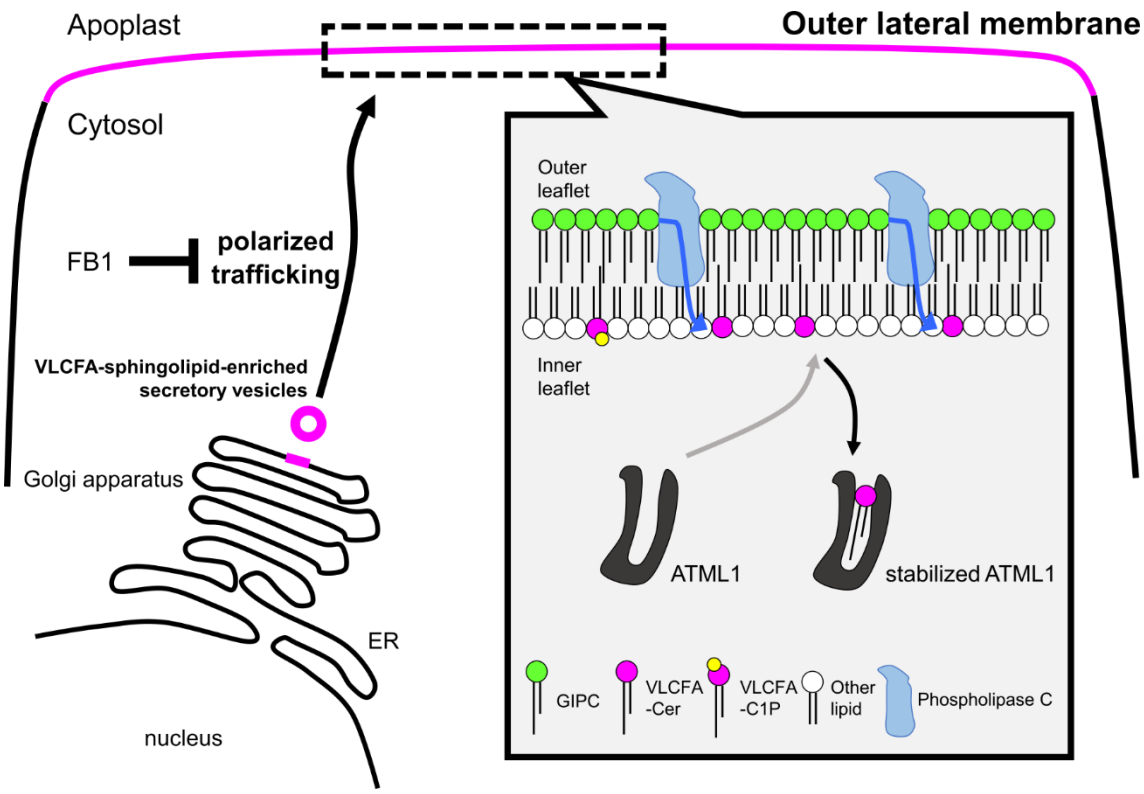

Fig. S13. Model of the polarized trafficking of VLCFA-sphingolipids to the outer lateral membrane and generation of VLCFA-Cers, which interact with intracellular ATML1.

VLCFA-sphingolipids are transported to the outer lateral membrane by a mechanism that is inhibited by FB1 treatment. Subsequently, VLCFA-sphingolipids (such as GIPCs) in the outer leaflet of the outer lateral membrane are hydrolyzed by specific enzymes (such as phospholipase C), generating VLCFA-Cers in the inner leaflet of the outer lateral membrane. Magenta line indicates apical membrane components. ER, endoplasmic reticulum.